AIMS Mathematics, 9(4): 8516–8563.
DOI: 10.3934/math.2024414
Received: 25 December 2023
Revised: 13 February 2024
Accepted: 19 February 2024
Published: 28 February 2024

http://www.aimspress.com/journal/Math

Research article

A mathematical model for fractal-fractional monkeypox disease and its application to real data

Weerawat Sudsutad[1], Chatthai Thaiprayoon[2], Jutarat Kongson[2,*] and Weerapan Sae-dan[3]

[1] Theoretical and Applied Data Integration Innovations Group, Department of Statistics, Faculty of Science, Ramkhamhaeng University, Bangkok 10240, Thailand; Email:weerawat.s@rumail.ru.ac.th

[2] Research Group of Theoretical and Computational Applied Science, Department of Mathematics, Faculty of Science, Burapha University, Chonburi 20131, Thailand; Email: chatthai@go.buu.ac.th

[3] Department of Computer Engineering, Faculty of Engineering, Ramkhamhaeng University, Bangkok 10240, Thailand; Email: weerapan.s@rumail.ru.ac.th

* **Correspondence:** Email: jutarat_k@go.buu.ac.th.

Abstract: In this paper, we developed a nonlinear mathematical model for the transmission of the monkeypox virus among populations of humans and rodents under the fractal-fractional operators in the context of Atangana-Baleanu. For the theoretical analysis, the renowned theorems of fixed points, like Banach's and Krasnoselskii's types, were used to prove the existence and uniqueness of the solutions. Additionally, some results regarding the stability of the equilibrium points and the basic reproduction number were provided. In addition, the numerical schemes of the considered model were established using the Adams-Bashforth method. Our analytical findings were supported by the numerical simulations to explain the effects of changing a few sets of fractional orders and fractal dimensions. Some graphic simulations were displayed with some parameters calculated from real data to understand the behavior of the model.

Keywords: monkeypox model; fractal-fractional operators; stability; existence and uniqueness; numerical Scheme
Mathematics Subject Classification: 26A33, 34A08, 65L09, 92D25, 92D30

1. Introduction

Although monkeypox has been extinct for a long while, it has been rediscovered recently. The disease has returned and is spreading to numerous nations worldwide. The WHO (World Health Organization) recently announced that the monkeypox ($\mathbb{MPX}$) epidemiological situation outbreak has returned in many countries. There have been numerous cases of monkeypox and clusters

reported concurrently in nonendemic and endemic states in a variety of geographical locations at this moment [1]. Retrace the history of MPX to about 60 years ago, when laboratory monkeys were first exposed to it as a viral zoonotic disease in 1958, and illnesses in humans were discovered in 1970 [2]. Many more MPX cases in Central and Western Africa have been revealed [3]. MPX is an infectious disease caused by the MPX virus within the Poxviridae family, which belongs to the class Orthopoxvirus [4–6]. The incubation period for MPX is typically 7–14 days but it can vary from 5–21 days. Transmission of the MPX virus emerges when an individual comes into contact with the virus from infected animals such as primates and rodents through bites or scratches, from humans by respiratory droplets, and contact with bodily fluids from a skin lesion on an infected individual, or from contaminated material with the virus. The symptoms of the MPX virus infection in humans are the same to the symptoms of smallpox, which usually include fever, headache, muscle aches, chills, weariness, and exhaustion, but monkeypox causes swollen lymph nodes while smallpox does not [7–9]. Presently, no standardized treatment is available for MPX infection but vaccination against smallpox can be used to reduce the risk of infection and provides approximately 85% protection against monkeypox. To prevent virus transmission, people with MPX should remain isolated for the duration of the illness [10–12].

In many branches of natural and applied sciences, scientists and researchers employ dynamical systems, which utilizes an important role in comprehending the dynamic behavior of real-world problems. Many researchers have areas of interest in modeling the diffuse of infectious diseases and the analysis of different factors related to the diffuse of disease, especially a current outbreak in which emergence and re-emergence of the crisis health like COVID-19 and MPX, respectively. In this study, some mathematical models related to MPX transmission have been created using a differential system. In 2011, Bhunu et al. [13] established the stability of the transmission dynamics of the MPX model. In 2017, They [14] provided a system of MPX viral infection transmission dynamics, together with a combined vaccine and treatment as control measures. Equilibrium points were establishedfor asymptote stability using the basic reproduction number. In 2019, Somma et al. [15] developed the model presented in [13] by including a quarantine group and a necessary factor in the human compartment to manage the transmission of the disease in the population. In 2020, Bankuru et al. [16] extended the work of [14] and evaluated individual and population-wide vaccination options in terms of cost and probabilistic disease acquisition using a game theoretical approach. In 2022, Peter et al. [17] discussed a system of the MPX virus. They proved asymptotic stability property for endemic and disease-free equilibriums on both local and global scales. For more examples, see [18–20].

Fractional calculus, which uses noninteger order instead of integer order, has been invented and developed to describe various complex model problems. It is commonly recognized that compared to traditional integer-order systems, noninteger-order systems give more accurate and reliable data since they have hereditary properties and a description of memory regarding the dynamics of many diseases. It is also a significant knowledge resource that has attracted the intention of many academics and researchers in solving the problems arising within the global environment. Some mathematicians have already introduced the various fractional derivatives offered in fractional calculus. The fractional operators are proposed according to the different kernels: The power kernel in the Liouville-Caputo operator, the exponential kernel in the Caputo-Fabrizio derivative, and the Mittag-Leffler kernel in the Atangana-Baleanu (AB) derivative operator [21–23]. Recently, Atangana [24] introduced differential and integral operators called fractal-fractional (FF) operators, which merges two orders of fractal

dimensions and fractional order of some kernels such as the power kernel, the exponential kernel, and the Mittag-Leffler kernel. In addition to fractional-order integration and differentiation, the advantage of using the $\mathbb{FF}$ operator is that it characterizes the current difficulties and challenges that arise in many problems that cannot be examined with classical operators. Some studies demonstrate that the $\mathbb{FF}$ operator is more realistic and helpful in utilizing mathematical model for real-world problems with real data than integer-order and fractional-order operators [25–27]. Many researchers study dynamical models related to the said operator, such as the epidemiology of HIV/AIDS model, the pandemic COVID-19 model, the spreading of malaria disease, the dynamics of the age-structure smoking model, etc.; the details can be found in [28–32].

According to the review of several articles on $\mathbb{MPX}$ virus infection, there is not much research on the spread of $\mathbb{MPX}$ virus with fractional-order operators. However, since the $\mathbb{MPX}$ returned in 2022, some researchers have given attention to studying and analyzing the $\mathbb{MPX}$ problems for controlling the $\mathbb{MPX}$ epidemic. For example, in 2022, Mesady et al. [38] formulated the fractional $\mathbb{MPX}$ model based on the Caputo's type derivative. The equilibrium points, the basic reproduction number, and the stability analysis were investigated in their work. Qurashi et al. [39] presented a fractional mathematical model within the $\mathbb{AB}$'s type derivative that depends on the Mittag-Leffler kernel. The stability of equilibria was examined. Peter et al. [40] studied and investigated the transmission dynamics and control of the fractional $\mathbb{MPX}$ infection model under the Caputo-Fabrizio's type derivative. For more works, see [33, 34]. Even though various researchers widely use fractional differential systems to solve real-world problems, it is pretty challenging to solve the exact solutions practically and solve the system of fractional derivatives analytically. Therefore, various famous and efficient techniques such as the Adams-Bashforth method [35, 36], the Newton polynomial approach [35, 36], and the predictor-corrector technique [36, 37] are usually used to solve the approximated solutions of the fractional differential systems. After composing all the stories and being inspired by the above discussions, the $\mathbb{FF}$ operator is very novel in this regard since it is the most recent operator, and there have not been a lot of literature-based studies on their usage. Additionally, in the sense of $\mathbb{FF}$ derivatives, it can explain the memory effect and fractal properties such as the fractional-order (α) and fractal-dimension (β), which are essential for explaining phenomena that occur in the real world. Fractals occur spontaneously in the majority of biological objects. As a consequence, two-dimensional epidemiological modeling accurately reflects the study's projections. The motivation for dealing with fractional systems in our proposed model is to address memory and hereditary criteria, which are complicated behavioral formats of biological systems. This allows us to construct a more realistic approach to biological systems. The memory function enables the proposed models with fractional order to integrate previously acquired information, resulting in more accurate predictions and translations. Therefore, we aim to study and analyze a model attended by fractional differential systems to establish memory's effect on the $\mathbb{MPX}$ model. To set our work apart from that of others, the $\mathbb{FF}$ operators in the $\mathbb{AB}$' type will be utilized in the classical model of $\mathbb{MPX}$ virus transmission among five groups of humans and three groups of rodents, which is formulated in [17] (we call this new model the $\mathbb{FF}$-$\mathbb{MPX}$ model). Here, the equilibrium points and their stability for the proposed model are established with the help of the basic reproduction number. The existence and uniqueness of the solutions are proven using many kinds of fixed-point theory, such as Banach's and Krasnoselskii's types. Finally, we use the fractional Adams-Bashforth method to obtain the approximated solutions to the proposed model. The numerical simulations are graphically shown to

study the evolution of the $\mathbb{FF}$-$\mathbb{MPX}$ model against different fractional-orders and fractal-dimensions. We provide critical qualitative data that will assist the government in establishing control actions for monkeypox caused by the monkeypox virus.

An overview of the major objectives explained in this paper is declared in the sections as follows: Section 2 presents some basic concepts of the $\mathbb{FF}$ operator in the $\mathbb{AB}$'s type, gives details of fixed-point theory and formulates the fractional $\mathbb{MPX}$ model via the Mittag-Leffler kernel. Section 3 discusses the positivity and equilibrium analysis of the $\mathbb{FF}$-$\mathbb{MPX}$ model. The fundamental properties and qualitative analysis of the proposed model is also discussed. The uniqueness result for the proposed model is demonstrated by applying Banach's fixed-point theorem. The existence result is established by employing Krasnoselskii's fixed-point theorem in Section 4. The numerical schemes using the Adams-Bashforth method for the $\mathbb{FF}$-$\mathbb{MPX}$ model are presented in Section 5. Moreover, Section 6 offers a discussion of some graphical illustrations to support the major results. The conclusion of the study is provided in the last section.

2. Preliminaries

2.1. Background materials

Now, we will introduce the foundational definitions of the $\mathbb{FF}$ operators that are used in this paper. Assume α is the fractional-order and β is the fractal-dimension. Suppose $y(t)$ is a continuous and fractal differentiable on (a,b) with β, then we have the following definitions defined as in [24, 41].

Definition 2.1. *[24] The $\mathbb{FF}$ derivative of the function $y(t)$ of order α and dimension β in the sense of Caputo with the Mittag-Leffler kernel is given by*

$$^{\mathbb{FFM}}\mathfrak{D}_{0,t}^{\alpha,\beta}y(t) = \frac{\mathbb{AB}(\alpha)}{1-\alpha}\int_a^t \mathbb{E}_\alpha\Big[-\frac{\alpha}{1-\alpha}(t-s)^\alpha\Big]\frac{dy(s)}{ds^\beta}ds, \quad t \geq a \geq 0, \tag{2.1}$$

where $\alpha,\ \beta \in (0,1]$, $\mathbb{AB}(\alpha) = 1-\alpha+\alpha/\Gamma(\alpha)$ is the normalization function with $\mathbb{AB}(0) = \mathbb{AB}(1) = 1$, and $dy(t)/dt^\beta = \lim_{s\to t}(y(s)-y(t))/(s^\beta - t^\beta)$. Moreover, the Mittag-Leffler function is defined by $\mathbb{E}_\alpha(z) = \sum_{k=0}^{\infty} z^k/\Gamma(\alpha k+1)$, $z,\ \alpha \in \mathbb{C}$, $\alpha > 0$, with $\mathbb{C}$ is the complex number set.

Definition 2.2. *[24, 41] The $\mathbb{FF}$ integral of $y(t)$ of order α and dimension β in the sense of Caputo with the Mittag-Leffler kernel is given by*

$$^{\mathbb{FFM}}\mathcal{I}_{0,t}^{\alpha,\beta}y(t) = \frac{\beta(1-\alpha)t^{\beta-1}y(t)}{\mathbb{AB}(\alpha)} + \frac{\alpha\beta}{\mathbb{AB}(\alpha)}\int_a^t (t-s)^{\alpha-1}s^{\beta-1}y(s)ds, \quad t \geq a \geq 0. \tag{2.2}$$

Definition 2.3. *[24] Let $y \in C((a,b),\mathbb{R})$, the fractal-Laplace transform of order $\beta > 0$ is given by*

$$^{\mathbb{F}}L_p^\beta y(t) = \int_0^\infty y(t)\exp(-pt)\,t^{\beta-1}dt. \tag{2.3}$$

Lemma 2.4. *[41] Consider the following $\mathbb{FF}$ initial value problem as follows:*

$$\begin{cases} ^{\mathbb{FFM}}\mathfrak{D}_{0,t}^{\alpha,\beta}y(t) = \mathbb{G}(t,y(t)), \quad t \in [0,T], \quad \alpha,\beta \in (0,1] \\ y(0) = y_0. \end{cases} \tag{2.4}$$

The problem (2.4) *can be written as [42]*

$$\begin{cases} {}^{\mathbb{FFM}}\mathfrak{D}_{0,t}^{\alpha,\beta} y(t) = \beta t^{\beta-1}\mathbb{G}(t, y(t)), \quad t \in [0, T], \quad \alpha, \beta \in (0, 1], \\ y(0) = y_0. \end{cases} \tag{2.5}$$

Hence, the solution of the problem (2.5) *is corresponding to the following integral equation*

$$y(t) = y(0) + \frac{\beta t^{\beta-1}(1-\alpha)\mathbb{G}(t, y(t))}{\mathbb{AB}(\alpha)} + \frac{\alpha\beta}{\mathbb{AB}(\alpha)\Gamma(\alpha)} \int_0^t s^{\beta-1}(t-s)^{\alpha-1}\mathbb{G}(s, y(s))ds. \tag{2.6}$$

The following lemmas are used to analyze the existence and uniqueness results of the proposed model.

Lemma 2.5. (Banach's Fixed Point Theorem [43]) *Assume* $\mathbb{X}$ *is a Banach space, and* $D \subset \mathbb{X}$, $D \neq \emptyset$ *is a closed subset. If the operator* $\mathcal{Q} : D \to D$ *holds the contraction condition, then* $\mathcal{Q}$ *has a unique fixed point in* D.

Lemma 2.6. (Krasnoselskii's Fixed Point Theorem [44]) *Assume* D *is a closed convex nonempty subset of a Banach space* $\mathbb{X}$. *Assume* $\mathcal{Q}$ *and* $\mathcal{P}$ *are two operators such that* (i). $\mathcal{Q}u + \mathcal{P}v \in D$, *whenever* u, $v \in D$; (ii). $\mathcal{P}$ *is compact and continuous;* (iii). $\mathcal{Q}$ *is contraction mapping. Then, there exists* $w \in D$ *such that* $z = \mathcal{Q}w + \mathcal{P}w$.

2.2. The $\mathbb{FF}$*-Order Extension of the* $\mathbb{MPX}$ *Model*

In this subsection, we first refer to the integer-order of the $\mathbb{MPX}$ model presented in [17], which studied the transmission dynamics of $\mathbb{MPX}$ consisting of five classes of humans and three classes of rodents, as shown in Figure 1.

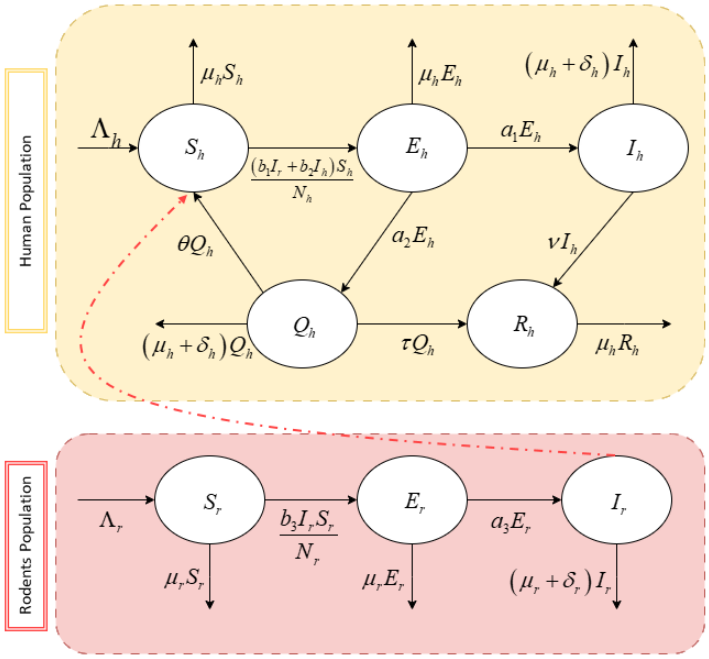

Figure 1. Transfer diagram of the $\mathbb{MPX}$ model.

They discussed the transmission dynamics of $\mathbb{MPX}$ in five classes of humans: Susceptible S_h, exposed E_h, infected I_h, isolated Q_h, recovered R_h, and three classes of rodents: Susceptible S_r, exposed E_r, and infected I_r. The $\mathbb{MPX}$ model is shown as the following

$$\begin{cases} \dfrac{dS_h(t)}{dt} = \Lambda_h - (b_1 I_r(t) + b_2 I_h(t))\dfrac{S_h(t)}{N_h(t)} - \mu_h S_h(t) + \theta Q_h(t), \\ \dfrac{dE_h(t)}{dt} = (b_1 I_r(t) + b_2 I_h(t))\dfrac{S_h(t)}{N_h(t)} - (a_1 + a_2 + \mu_h)E_h(t), \\ \dfrac{dI_h(t)}{dt} = a_1 E_h(t) - (\mu_h + \delta_h + \nu)I_h(t), \\ \dfrac{dQ_h(t)}{dt} = a_2 E_h(t) - (\theta + \tau + \delta_h + \mu_h)Q_h(t), \\ \dfrac{dR_h(t)}{dt} = \nu I_h(t) + \tau Q_h(t) - \mu_h R_h(t), \\ \dfrac{dS_r(t)}{dt} = \Lambda_r - b_3\dfrac{S_r(t)I_r(t)}{N_r(t)} - \mu_r S_r(t), \\ \dfrac{dE_r(t)}{dt} = b_3\dfrac{S_r(t)I_r(t)}{N_r(t)} - (\mu_r + a_3)E_r(t), \\ \dfrac{dI_r(t)}{dt} = a_3 E_r(t) - (\mu_r + \delta_r)I_r(t), \end{cases} \tag{2.7}$$

where the human class, $N_h = S_h + E_h + I_h + Q_h + R_h$, and the rodent class $N_r = S_r + E_r + I_r$, with the positive initial conditions $S_h(0) = S_{h_0} \geq 0$, $E_h(0) = E_{h_0} \geq 0$, $I_h(0) = I_{h_0} \geq 0$, $Q_h(0) = Q_{h_0} \geq 0$, $R_h(0) = R_{h_0} \geq 0$, $S_r(0) = S_{r_0} \geq 0$, $E_r(0) = E_{r_0} \geq 0$, $I_r(0) = I_{r_0} \geq 0$. The descriptions of all parameters are shown in Table 1.

Table 1. The descriptions of all parameters for the $\mathbb{MPX}$ model (2.7).

Parameters	Descriptions
Λ_h, Λ_r	The recruitment rate for susceptible humans and rodents, respectively.
b_1, b_3	The rate of rodent contact with humans and rodents, respectively.
b_2	The rate of human contact with humans.
a_1	The proportion of exposed humans to infected humans.
a_2	Proportion identified as the suspected case.
θ	Proportion not detected after diagnosis.
τ	Progression from isolated to recovered class.
ν	The rate of recovery for humans.
μ_h, μ_r	Natural death rate of humans and rodents, respectively.
δ_h, δ_r	Disease induced death rate for humans and rodents, respectively.

Now, we further develop the $\mathbb{MPX}$ model (2.7) utilizing the $\mathbb{FF}$ derivative operator in the context of the Mittag-Leffler kernel of order $\alpha \in (0, 1]$ and $\beta \in [0, 1]$, ${}^{\mathbb{FFM}}\mathfrak{D}_{0,t}^{\alpha,\beta}$, as follows:

$$\begin{cases} {}^{\mathbb{FFM}}\mathfrak{D}_{0,t}^{\alpha,\beta} S_h(t) = \mathbb{G}_1(t, S_h(t), E_h(t), I_h(t), R_h(t), Q_h(t), S_r(t), E_r(t), I_r(t)), \\ {}^{\mathbb{FFM}}\mathfrak{D}_{0,t}^{\alpha,\beta} E_h(t) = \mathbb{G}_2(t, S_h(t), E_h(t), I_h(t), R_h(t), Q_h(t), S_r(t), E_r(t), I_r(t)), \\ {}^{\mathbb{FFM}}\mathfrak{D}_{0,t}^{\alpha,\beta} I_h(t) = \mathbb{G}_3(t, S_h(t), E_h(t), I_h(t), R_h(t), Q_h(t), S_r(t), E_r(t), I_r(t)), \\ {}^{\mathbb{FFM}}\mathfrak{D}_{0,t}^{\alpha,\beta} Q_h(t) = \mathbb{G}_4(t, S_h(t), E_h(t), I_h(t), R_h(t), Q_h(t), S_r(t), E_r(t), I_r(t)), \\ {}^{\mathbb{FFM}}\mathfrak{D}_{0,t}^{\alpha,\beta} R_h(t) = \mathbb{G}_5(t, S_h(t), E_h(t), I_h(t), R_h(t), Q_h(t), S_r(t), E_r(t), I_r(t)), \\ {}^{\mathbb{FFM}}\mathfrak{D}_{0,t}^{\alpha,\beta} S_r(t) = \mathbb{G}_6(t, S_h(t), E_h(t), I_h(t), R_h(t), Q_h(t), S_r(t), E_r(t), I_r(t)), \\ {}^{\mathbb{FFM}}\mathfrak{D}_{0,t}^{\alpha,\beta} E_r(t) = \mathbb{G}_7(t, S_h(t), E_h(t), I_h(t), R_h(t), Q_h(t), S_r(t), E_r(t), I_r(t)), \\ {}^{\mathbb{FFM}}\mathfrak{D}_{0,t}^{\alpha,\beta} I_r(t) = \mathbb{G}_8(t, S_h(t), E_h(t), I_h(t), R_h(t), Q_h(t), S_r(t), E_r(t), I_r(t)), \end{cases} \tag{2.8}$$

where $\mathbb{G}_i = \mathbb{G}_i(t, S_h(t), E_h(t), I_h(t), R_h(t), Q_h(t), S_r(t), E_r(t), I_r(t))$, for $i = 1, 2, \ldots, 8$ and the functions $\mathbb{G}_i$ for the developed model is defined as below:

$$\begin{cases} \mathbb{G}_1 = \Lambda_h - (b_1 I_r(t) + b_2 I_h(t))\dfrac{S_h(t)}{N_h(t)} - \mu_h S_h(t) + \theta Q_h(t), \\ \mathbb{G}_2 = (b_1 I_r(t) + b_2 I_h(t))\dfrac{S_h(t)}{N_h(t)} - (a_1 + a_2 + \mu_h) E_h(t), \\ \mathbb{G}_3 = a_1 E_h(t) - (\mu_h + \delta_h + \nu) I_h(t), \\ \mathbb{G}_4 = a_2 E_h(t) - (\theta + \tau + \delta_h + \mu_h) Q_h(t), \\ \mathbb{G}_5 = \nu I_h(t) + \tau Q_h(t) - \mu_h R_h(t), \\ \mathbb{G}_6 = \Lambda_r - b_3 \dfrac{S_r(t) I_r(t)}{N_r(t)} - \mu_r S_r(t), \\ \mathbb{G}_7 = b_3 \dfrac{S_r(t) I_r(t)}{N_r(t)} - (\mu_r + a_3) E_r(t), \\ \mathbb{G}_8 = a_3 E_r(t) - (\mu_r + \delta_r) I_r(t), \end{cases} \tag{2.9}$$

with $S_{h_0} \geq 0$, $E_{h_0} \geq 0$, $I_{h_0} \geq 0$, $Q_{h_0} \geq 0$, $R_{h_0} \geq 0$, $S_{r_0} \geq 0$, $E_{r_0} \geq 0$, and $I_{r_0} \geq 0$. The model (2.8) is called the $\mathbb{FF}$-$\mathbb{MPX}$ model. Notice that if we set $\alpha = 1$ in the $\mathbb{FF}$-$\mathbb{MPX}$ model, then it reduces to the $\mathbb{MPX}$ model (2.7), which provides the integer-order model. Furthermore, it can be reduced to the fractional $\mathbb{MPX}$ model by setting $\beta = 1$.

3. Model analysis

This section highlights the positiveness and equilibrium analysis of $\mathbb{FF}$-$\mathbb{MPX}$ model (2.8).

3.1. Positiveness of the model

For the positiveness and boundedness of the $\mathbb{FF}$-$\mathbb{MPX}$ model, we set $\mathbb{R}_+^8 = \{\mathbb{G} \in \mathbb{R}^8 : \mathbb{G} \geq 0$ and $\mathbb{G} = \left(S_h, E_h, I_h, Q_h, R_h, S_r, E_r, I_r\right)^{\mathcal{T}}\}$, where $(\cdot)^{\mathcal{T}}$ is the vector transpose.

Theorem 3.1. *The solution* $\mathbb{G}$ *for the* $\mathbb{FF}$-$\mathbb{MPX}$ *model* (2.8) *is unique and bounded in* $\mathbb{R}_+^8$. *Moreover, the solution will be non-negative.*

Proof. For $t \in (0, \infty)$, we obtain its existence and uniqueness of the $\mathbb{FF}$-$\mathbb{MPX}$ model (2.8). Subsequently, we will present that the non-negative region $\mathbb{R}_+^8$ is a positive invariant region. Using

the $\mathbb{FF}$-$\mathbb{MPX}$ model (2.8), we get

$$\begin{cases} {}^{\mathbb{FFM}}\mathfrak{D}_{0,t}^{\alpha,\beta} S_h(t) = \Lambda_h + \theta Q_h(t) \geq 0, \\ {}^{\mathbb{FFM}}\mathfrak{D}_{0,t}^{\alpha,\beta} E_h(t) = \dfrac{(b_1 I_r(t) + b_2 I_h(t)) S_h(t)}{N_h(t)} \geq 0, \\ {}^{\mathbb{FFM}}\mathfrak{D}_{0,t}^{\alpha,\beta} I_h(t) = a_1 E_h(t) \geq 0, \\ {}^{\mathbb{FFM}}\mathfrak{D}_{0,t}^{\alpha,\beta} Q_h(t) = a_2 E_h(t) \geq 0, \\ {}^{\mathbb{FFM}}\mathfrak{D}_{0,t}^{\alpha,\beta} R_h(t) = \nu I_h(t) + \tau Q_h(t) \geq 0, \\ {}^{\mathbb{FFM}}\mathfrak{D}_{0,t}^{\alpha,\beta} S_r(t) = \Lambda_r \geq 0, \\ {}^{\mathbb{FFM}}\mathfrak{D}_{0,t}^{\alpha,\beta} E_r(t) = \dfrac{b_3 S_r(t) I_r(t)}{N_r(t)} \geq 0, \\ {}^{\mathbb{FFM}}\mathfrak{D}_{0,t}^{\alpha,\beta} I_r(t) = a_3 E_r(t) \geq 0. \end{cases} \tag{3.1}$$

If $(S_{h_0}, E_{h_0}, I_{h_0}, Q_{h_0}, R_{h_0}, S_{r_0}, E_{r_0}, I_{r_0}) \in \mathbb{R}_+^8$, then according to (3.1) the solution $\mathbb{G}$ cannot escape from the hyperplanes. Consequently, $\mathbb{R}_+^8$ is a positive invariant set. Since the total population of humans and rodents are $N_h = S_h + E_h + I_h + Q_h + R_h$, and $N_r = S_r + E_r + I_r$. So, from the $\mathbb{FF}$-$\mathbb{MPX}$ model (2.8), we can obtain that

$$\begin{cases} {}^{\mathbb{FFM}}\mathfrak{D}_{0,t}^{\alpha,\beta} N_h(t) \leq \Lambda_h - \mu_h N_h(t), \\ {}^{\mathbb{FFM}}\mathfrak{D}_{0,t}^{\alpha,\beta} N_r(t) \leq \Lambda_r - \mu_r N_r(t). \end{cases} \tag{3.2}$$

Utilizing the fractal Laplace transform (2.3), leads to the conclusion that $N_h \leq \Lambda_h/\mu_h$ and $N_r \leq \Lambda_r/\mu_r$ as $t \to \infty$. Therefore, we obtain the biologically feasible region of the $\mathbb{FF}$-$\mathbb{MPX}$ model (2.8) as follows:

$$\begin{aligned} \mathfrak{A}_1 &= \left\{ (S_h, E_h, I_h, Q_h, R_h) \in \mathbb{R}^5 : S_h, E_h, I_h, Q_h, R_h \geq 0 \quad \text{and} \quad N_h \leq \frac{\Lambda_h}{\mu_h} \right\}, \\ \mathfrak{A}_2 &= \left\{ (S_r, E_r, I_r) \in \mathbb{R}^3 : S_r, E_r, I_r \geq 0 \quad \text{and} \quad N_r \leq \frac{\Lambda_r}{\mu_r} \right\}. \end{aligned}$$

The proof is completed. □

3.2. Equilibrium points and their stability

The $\mathbb{FF}$-$\mathbb{MPX}$ model (2.8) has two steady states that will be obtained by taking the right side of (2.8) equal to zero. Then we get

- The disease-free equilibrium $\mathfrak{E}_0^* = (S_{h_0}^*, E_{h_0}^*, I_{h_0}^*, Q_{h_0}^*, R_{h_0}^*, S_{r_0}^*, E_{r_0}^*, I_{r_0}^*) = (\frac{\Lambda_h}{\mu_h}, 0, 0, 0, 0, \frac{\Lambda_r}{\mu_r}, 0, 0)$.
- The endemic equilibrium $\mathfrak{E}_1^* = (S_h^*, E_h^*, I_h^*, Q_h^*, R_h^*, S_r^*, E_r^*, I_r^*)$, where

$$\begin{aligned} S_h^* &= \frac{K_1 K_3 N_h \Lambda_h}{(K_1 K_3 - \theta a_2)(b_1 I_r^* + b_2 I_h^*) + K_1 K_3 \mu_h N_h}, & E_h^* &= \frac{K_2 I_h^*}{a_1}, \\ I_h^* &= \frac{\phi + \sqrt{\phi^2 + 4K_2(K_1 K_3 - \theta a_2)(a_1 b_1 b_2 K_3 \Lambda_h I_r^*)}}{2b_2 K_2 (K_1 K_3 - \theta a_2)}, & Q_h^* &= \frac{a_2 K_2 I_h^*}{a_1 K_3}, \\ R_h^* &= \frac{(a_1 \nu K_3 + \tau K_2 a_2) I_h^*}{a_1 K_3 \mu_h}, \quad S_r^* = \frac{N_r K_4 K_5}{a_3 b_3}, \quad E_r^* = \frac{K_4 I_r^*}{a_3}, \quad I_r^* = \frac{a_3 b_3 \Lambda_r - K_4 K_5 N_r \mu_r}{K_4 K_5 b_3}, \end{aligned}$$

where $K_1 = a_1 + a_2 + \mu_h, K_2 = \mu_h + \delta_h + \nu, K_3 = \theta + \tau + \delta_h + \mu_h$, $K_4 = \mu_r + \delta_r$, $K_5 = \mu_r + a_3$ and $\phi = a_1K_3\Lambda_h b_2 - b_1K_2I_r^*(K_1K_3 - \theta a_2) - K_1K_2K_3\mu_h N_h$. To examine the stability of the equilibrium points, we first apply the next-generation matrix method [45] for the $\mathbb{FF}$-$\mathbb{MPX}$ model (2.8) to find the basic reproduction number ($\Re_0$). For this purpose, we will focus solely on the infectious populations of the proposed model, i.e., E_h, I_h, Q_h and I_r. So, the transmission matrix (F) and the transitions matrix (V) can be determined as:

$$F = \begin{pmatrix} 0 & b_2 & 0 & b_1 \\ 0 & 0 & 0 & 0 \\ 0 & 0 & 0 & 0 \\ 0 & 0 & 0 & 0 \end{pmatrix} \quad \text{and} \quad V = \begin{pmatrix} K_1 & 0 & 0 & 0 \\ -a_1 & K_2 & 0 & 0 \\ -a_2 & 0 & K_3 & 0 \\ 0 & 0 & 0 & K_4 \end{pmatrix}.$$

This yields the next-generation matrix as below:

$$FV^{-1} = \begin{pmatrix} \frac{a_1b_2}{K_1K_2} & \frac{b_2}{K_2} & 0 & \frac{b_1}{K_4} \\ 0 & 0 & 0 & 0 \\ 0 & 0 & 0 & 0 \\ 0 & 0 & 0 & 0 \end{pmatrix}. \tag{3.3}$$

Hence, the spectral radius of (3.3) represented by $\Re_0 = \rho(FV^{-1})$ can be obtained as

$$\Re_0 = \frac{a_1b_2}{K_1K_2} = \frac{a_1b_2}{(a_1 + a_2 + \mu_h)(\mu_h + \delta_h + \nu)}. \tag{3.4}$$

Next, we establish the assumptions for the stability of the disease-free equilibrium.

Theorem 3.2. *The disease-free equilibrium $\mathfrak{E}_0^*$ of the $\mathbb{FF}$-$\mathbb{MPX}$ model* (2.8) *is locally asymptotically stable whenever $K_4K_5 > a_3b_3$ and $\Re_0 < 1$, with the necessary and sufficient conditions:*

$$|arg(\lambda_i)| > \frac{\alpha\pi}{2}, \quad i = 1, 2, \ldots, 8. \tag{3.5}$$

Proof. To discuss the stability criterion of $\mathfrak{E}_0^*$, the general Jacobian matrix of the $\mathbb{FF}$-$\mathbb{MPX}$ model (2.8) at $\mathfrak{E}_0^*$ has been obtained as follows

$$J(\mathfrak{E}_0^*) = \begin{pmatrix} -\mu_h & 0 & -b_2 & \theta & 0 & 0 & 0 & -b_1 \\ 0 & -K_1 & b_2 & 0 & 0 & 0 & 0 & b_1 \\ 0 & a_1 & -K_2 & 0 & 0 & 0 & 0 & 0 \\ 0 & a_2 & 0 & -K_3 & 0 & 0 & 0 & 0 \\ 0 & 0 & \nu & \tau & -\mu_h & 0 & 0 & 0 \\ 0 & 0 & 0 & 0 & 0 & -\mu_r & 0 & -b_3 \\ 0 & 0 & 0 & 0 & 0 & 0 & -K_5 & b_3 \\ 0 & 0 & 0 & 0 & 0 & 0 & a_3 & -K_4 \end{pmatrix}.$$

The eigenvalues $\lambda_i, i = 1, 2, \ldots, 8$ can be calculated by solving the characteristic equation $|J(\mathfrak{E}_0^*) - \lambda\hat{I}| = 0$ where $\hat{I}$ is an identity matrix. So, we get

$$(\lambda + \mu_h)^2(\lambda + K_3)(\lambda + \mu_r)[(\lambda + K_4)(\lambda + K_5) - a_3b_3][(\lambda + K_1)(\lambda + K_2) - a_1b_2] = 0. \tag{3.6}$$

Thus, the eigenvalues of $J(\mathfrak{E}_0)$ are given by

$$\begin{aligned}
\lambda_1 &= -\mu_h, \quad \lambda_2 = -\mu_h, \quad \lambda_3 = -K_3, \quad \lambda_4 = -\mu_r, \\
\lambda_{5,6} &= \frac{-(K_4+K_5) \pm \sqrt{(K_4+K_5)^2 - 4(K_4K_5 - a_3b_3)}}{2}, \\
\lambda_{7,8} &= \frac{-(K_1+K_2) \pm \sqrt{(K_1+K_2)^2 - 4K_1K_2(1-\Re)}}{2}.
\end{aligned}$$

It is easy to see that $\lambda_{5,6} < 0$ if $K_4K_5 > a_3b_3$ and $\lambda_{7,8} < 0$ if $\Re < 1$. Hence, all roots of (3.6) have negative real parts, which guarantees the inequality of (3.5) for all $\alpha \in (0,1]$. Hence, the point $\mathfrak{E}_0^*$ is locally asymptotically stable. The proof is done. □

Now, we will analyze the stability of the endemic equilibrium $(\mathfrak{E}_1^*)$ by employing the Routh-Hurwitz criterion to demonstrate the locally asymptotically stable. The general Jacobian matrix of the $\mathbb{FF}$-$\mathbb{MPX}$ model (2.8) at $\mathfrak{E}_1^*$ is provided as follows

$$J(\mathfrak{E}_1^*) = \begin{pmatrix}
-\left(\frac{b_1I_r+b_2I_h}{N_h}\right) - \mu_h & 0 & \frac{-b_2S_h}{N_h} & \theta & 0 & 0 & 0 & \frac{-b_1S_h}{N_h} \\
\left(\frac{b_1I_r+b_2I_h}{N_h}\right) & -K_1 & \frac{b_2S_h}{N_h} & 0 & 0 & 0 & 0 & \frac{b_1S_h}{N_h} \\
0 & a_1 & -K_2 & 0 & 0 & 0 & 0 & 0 \\
0 & a_2 & 0 & -K_3 & 0 & 0 & 0 & 0 \\
0 & 0 & \nu & \tau & -\mu_h & 0 & 0 & 0 \\
0 & 0 & 0 & 0 & 0 & \frac{-b_3I_r}{N_r} - \mu_r & 0 & \frac{-b_3S_r}{N_r} \\
0 & 0 & 0 & 0 & 0 & \frac{b_3I_r}{N_r} & -K_5 & \frac{b_3S_r}{N_r} \\
0 & 0 & 0 & 0 & 0 & 0 & a_3 & -K_4
\end{pmatrix}.$$

It is easy to see that one eigenvalue obtained from the characteristic equation of $J(\mathfrak{E}_1^*)$ is $\omega_1 = -\mu_h$, which is a negative value. Therefore, the local stability of $\mathfrak{E}_1^*$ demands the negative real parts of all roots of the equation

$$\omega^7 + \mathcal{A}_1\omega^6 + \mathcal{A}_2\omega^5 + \mathcal{A}_3\omega^4 + \mathcal{A}_4\omega^3 + \mathcal{A}_5\omega^2 + \mathcal{A}_6\omega + \mathcal{A}_7 = 0, \tag{3.7}$$

where $\mathcal{A}_j$ are the coefficients of ω^{7-j}, $j = 1, 2, \ldots, 7$, after rearranging the polynomial equation in standard form. Afterwards, to achieve the $\mathfrak{E}_1^*$ stability, we present the parameters below:

$$\begin{aligned}
\mathcal{B}_1 &= \frac{\mathcal{A}_1\mathcal{A}_2 - \mathcal{A}_3}{\mathcal{A}_1}, \quad \mathcal{B}_2 = \frac{\mathcal{A}_1\mathcal{A}_4 - \mathcal{A}_5}{\mathcal{A}_1}, \quad \mathcal{B}_3 = \frac{\mathcal{A}_1\mathcal{A}_6 - \mathcal{A}_7}{\mathcal{A}_1}, \quad \mathcal{C}_1 = \frac{\mathcal{A}_3\mathcal{B}_1 - \mathcal{A}_1\mathcal{B}_2}{\mathcal{B}_1}, \\
\mathcal{C}_2 &= \frac{\mathcal{A}_5\mathcal{B}_1 - \mathcal{A}_1\mathcal{B}_3}{\mathcal{B}_1}, \quad \mathcal{C}_3 = \mathcal{A}_7, \quad \mathcal{D}_1 = \frac{\mathcal{B}_2\mathcal{C}_1 - \mathcal{B}_1\mathcal{C}_2}{\mathcal{C}_1}, \quad \mathcal{D}_2 = \frac{\mathcal{B}_3\mathcal{C}_1 - \mathcal{B}_1\mathcal{C}_3}{\mathcal{C}_1}, \\
\mathcal{E}_1 &= \frac{\mathcal{C}_2\mathcal{D}_1 - \mathcal{C}_1\mathcal{D}_2}{\mathcal{D}_1}, \quad \mathcal{E}_2 = \mathcal{C}_3, \quad \mathcal{F}_1 = \frac{\mathcal{D}_2\mathcal{E}_1 - \mathcal{D}_1\mathcal{E}_2}{\mathcal{E}_1}.
\end{aligned}$$

Hence, the Routh-Hurwitz conditions for confirming the negative real parts of all roots of (3.7) are presented, and the local stability of $\mathfrak{E}_1^*$ is concluded in the following theorem:

Theorem 3.3. *The endemic equilibrium $\mathfrak{E}_1^*$ of the $\mathbb{FF}$-$\mathbb{MPX}$ model (2.8) is locally asymptotically stable whenever the necessary and sufficient conditions below are satisfied: (i) $\mathcal{A}_1 > 0$; (ii) $\mathcal{A}_7 > 0$, (iii) $\mathcal{A}_1\mathcal{A}_2 > \mathcal{A}_3$, (iv) $\mathcal{A}_1\mathcal{A}_2\mathcal{A}_3 + \mathcal{A}_1\mathcal{A}_5 > \mathcal{A}_1^2\mathcal{A}_4 + \mathcal{A}_3^2$, (v) $\mathcal{B}_2\mathcal{C}_1 > \mathcal{B}_1\mathcal{C}_2$, (vi) $\mathcal{C}_2\mathcal{D}_1 > \mathcal{C}_1\mathcal{D}_2$, (vii) $\mathcal{D}_2\mathcal{E}_1 > \mathcal{D}_1\mathcal{E}_2$.*

4. Qualitative analysis of the $\mathbb{FF}$-$\mathbb{MPX}$ model

To demonstrate the qualitative results of the $\mathbb{FF}$-$\mathbb{MPX}$ model (2.8), we give a Banach space on $\mathcal{J} := [0, T]$ of all continuous real-valued functions denoted as $\mathbb{X} = C(\mathcal{J} \times \mathbb{R}^8, \mathbb{R})$ equipped with the norms $\|\mathcal{Y}\| = \|(S_h, E_h, I_h, Q_h, R_h, S_r, E_r, I_r)\| = \|S_h\| + \|E_h\| + \|I_h\| + \|Q_h\| + \|R_h\| + \|S_r\| + \|E_r\| + \|I_r\|$, $\|S_h\| = \sup_{t\in\mathcal{J}} |S_h(t)| = \mathfrak{B}_{h_1}$, $\|E_h\| = \sup_{t\in\mathcal{J}} |E_h(t)| = \mathfrak{B}_{h_2}$, $\|I_h\| = \sup_{t\in\mathcal{J}} |I_h(t)| = \mathfrak{B}_{h_3}$, $\|Q_h\| = \sup_{t\in\mathcal{J}} |Q_h(t)| = \mathfrak{B}_{h_4}$, $\|R_h\| = \sup_{t\in\mathcal{J}} |R_h(t)| = \mathfrak{B}_{h_5}$, $\|S_r\| = \sup_{t\in\mathcal{J}} |S_r(t)| = \mathfrak{B}_{r_1}$, $\|E_r\| = \sup_{t\in\mathcal{J}} |E_r(t)| = \mathfrak{B}_{r_2}$, $\|I_r\| = \sup_{t\in\mathcal{J}} |I_r(t)| = \mathfrak{B}_{r_3}$, where $S_h, E_h, I_h, Q_h, R_h, S_r, E_r, I_r \in \mathbb{X}$.

Lemma 4.1. *Let $\mathbb{G} \in \mathbb{X}$ and $\mathcal{Y} \in C(\mathcal{J}, \mathbb{R})$, then the $\mathbb{FF}$-$\mathbb{MPX}$ model* (2.8) *which can be written as*

$$\begin{cases} {}^{\mathbb{FFM}}\mathfrak{D}_{0,t}^{\alpha,\beta}\mathcal{Y}(t) = \mathbb{G}(t, \mathcal{Y}(t)), \quad t \in [0, T], \quad \alpha, \beta \in (0, 1], \\ \mathcal{Y}(0) = \mathcal{Y}_0, \end{cases} \tag{4.1}$$

where

$$\mathcal{Y}(t) = \begin{pmatrix} S_h(t) \\ E_h(t) \\ I_h(t) \\ R_h(t) \\ Q_h(t) \\ S_r(t) \\ E_r(t) \\ I_r(t) \end{pmatrix}, \qquad \mathcal{Y}(0) = \begin{pmatrix} S_h(0) \\ E_h(0) \\ I_h(0) \\ R_h(0) \\ Q_h(0) \\ S_r(0) \\ E_r(0) \\ I_r(0) \end{pmatrix}, \qquad \mathbb{G}(t, \mathcal{Y}(t)) = \begin{pmatrix} \mathbb{G}_1(t, S_h(t)) \\ \mathbb{G}_2(t, E_h(t)) \\ \mathbb{G}_3(t, I_h(t)) \\ \mathbb{G}_4(t, R_h(t)) \\ \mathbb{G}_5(t, Q_h(t)) \\ \mathbb{G}_6(t, S_r(t)) \\ \mathbb{G}_7(t, E_r(t)) \\ \mathbb{G}_8(t, I_r(t)) \end{pmatrix}, \tag{4.2}$$

when $\mathbb{G}_i$, $i = 1, 2, \ldots, 8$, are given by (2.9)*. By applying* (2.5)*, the solution of the problem* (4.1) *is corresponding to the following integral equation*

$$\mathcal{Y}(t) = \mathcal{Y}(0) + \frac{\beta t^{\beta-1}(1-\alpha)\mathbb{G}(t, \mathcal{Y}(t))}{\mathbb{AB}(\alpha)} + \frac{\alpha\beta}{\mathbb{AB}(\alpha)\Gamma(\alpha)} \int_0^t s^{\beta-1}(t-s)^{\alpha-1}\mathbb{G}(s, \mathcal{Y}(s))ds. \tag{4.3}$$

For ease of calculation throughout this work, we provide the symbols

$$\begin{cases} \mathbb{G}_1(t, S_h(t)) = \mathbb{G}_1(t, S_h(t), E_h(t), I_h(t), Q_h(t), R_h(t), S_r(t), E_r(t), I_r(t)), \\ \mathbb{G}_2(t, E_h(t)) = \mathbb{G}_2(t, S_h(t), E_h(t), I_h(t), Q_h(t), R_h(t), S_r(t), E_r(t), I_r(t)), \\ \mathbb{G}_3(t, I_h(t)) = \mathbb{G}_3(t, S_h(t), E_h(t), I_h(t), Q_h(t), R_h(t), S_r(t), E_r(t), I_r(t)), \\ \mathbb{G}_4(t, Q_h(t)) = \mathbb{G}_4(t, S_h(t), E_h(t), I_h(t), Q_h(t), R_h(t), S_r(t), E_r(t), I_r(t)), \\ \mathbb{G}_5(t, R_h(t)) = \mathbb{G}_5(t, S_h(t), E_h(t), I_h(t), Q_h(t), R_h(t), S_r(t), E_r(t), I_r(t)), \\ \mathbb{G}_6(t, S_r(t)) = \mathbb{G}_6(t, S_h(t), E_h(t), I_h(t), Q_h(t), R_h(t), S_r(t), E_r(t), I_r(t)), \\ \mathbb{G}_7(t, E_r(t)) = \mathbb{G}_7(t, S_h(t), E_h(t), I_h(t), Q_h(t), R_h(t), S_r(t), E_r(t), I_r(t)), \\ \mathbb{G}_8(t, I_r(t)) = \mathbb{G}_8(t, S_h(t), E_h(t), I_h(t), Q_h(t), R_h(t), S_r(t), E_r(t), I_r(t)). \end{cases} \tag{4.4}$$

From Lemma 4.1, the $\mathbb{FF}$-$\mathbb{MPX}$ model (2.8) is corresponding the following Volterra integral equations as

$$S_h(t) = S_h(0) + \frac{\beta t^{\beta-1}(1-\alpha)\mathbb{G}_1(t, S_h(t))}{\mathbb{AB}(\alpha)}$$

$$+\frac{\alpha\beta}{\mathbb{AB}(\alpha)\Gamma(\alpha)}\int_0^t s^{\beta-1}(t-s)^{\alpha-1}\mathbb{G}_1(s,S_h(s))ds, \tag{4.5}$$

$$E_h(t) = E_h(0)+\frac{\beta t^{\beta-1}(1-\alpha)\mathbb{G}_2(t,E_h(t))}{\mathbb{AB}(\alpha)} +\frac{\alpha\beta}{\mathbb{AB}(\alpha)\Gamma(\alpha)}\int_0^t s^{\beta-1}(t-s)^{\alpha-1}\mathbb{G}_2(s,E_h(s))ds, \tag{4.6}$$

$$I_h(t) = I_h(0)+\frac{\beta t^{\beta-1}(1-\alpha)\mathbb{G}_3(t,I_h(t))}{\mathbb{AB}(\alpha)} +\frac{\alpha\beta}{\mathbb{AB}(\alpha)\Gamma(\alpha)}\int_0^t s^{\beta-1}(t-s)^{\alpha-1}\mathbb{G}_3(s,I_h(s))ds, \tag{4.7}$$

$$Q_h(t) = Q_h(0)+\frac{\beta t^{\beta-1}(1-\alpha)\mathbb{G}_4(t,Q_h(t))}{\mathbb{AB}(\alpha)} +\frac{\alpha\beta}{\mathbb{AB}(\alpha)\Gamma(\alpha)}\int_0^t s^{\beta-1}(t-s)^{\alpha-1}\mathbb{G}_4(s,Q_h(s))ds, \tag{4.8}$$

$$R_h(t) = R_h(0)+\frac{\beta t^{\beta-1}(1-\alpha)\mathbb{G}_5(t,R_h(t))}{\mathbb{AB}(\alpha)} +\frac{\alpha\beta}{\mathbb{AB}(\alpha)\Gamma(\alpha)}\int_0^t s^{\beta-1}(t-s)^{\alpha-1}\mathbb{G}_5(s,R_h(s))ds, \tag{4.9}$$

$$S_r(t) = S_r(0)+\frac{\beta t^{\beta-1}(1-\alpha)\mathbb{G}_6(t,S_r(t))}{\mathbb{AB}(\alpha)} +\frac{\alpha\beta}{\mathbb{AB}(\alpha)\Gamma(\alpha)}\int_0^t s^{\beta-1}(t-s)^{\alpha-1}\mathbb{G}_6(s,S_r(s))ds, \tag{4.10}$$

$$E_r(t) = E_r(0)+\frac{\beta t^{\beta-1}(1-\alpha)\mathbb{G}_7(t,E_r(t))}{\mathbb{AB}(\alpha)} +\frac{\alpha\beta}{\mathbb{AB}(\alpha)\Gamma(\alpha)}\int_0^t s^{\beta-1}(t-s)^{\alpha-1}\mathbb{G}_7(s,E_r(s))ds, \tag{4.11}$$

$$I_r(t) = I_r(0)+\frac{\beta t^{\beta-1}(1-\alpha)\mathbb{G}_8(t,I_r(t))}{\mathbb{AB}(\alpha)} +\frac{\alpha\beta}{\mathbb{AB}(\alpha)\Gamma(\alpha)}\int_0^t s^{\beta-1}(t-s)^{\alpha-1}\mathbb{G}_8(s,I_r(s))ds. \tag{4.12}$$

In view of (4.5)–(4.12), we define an operator $\mathcal{T} : \mathbb{X} \to \mathbb{X}$, where $\mathcal{T} = (\mathcal{T}_1,\mathcal{T}_2,\mathcal{T}_3,\mathcal{T}_4,\mathcal{T}_5,\mathcal{T}_6,\mathcal{T}_7,\mathcal{T}_8)$,

$$(\mathcal{T}_1S_h)(t) = S_h(0)+\frac{\beta t^{\beta-1}(1-\alpha)\mathbb{G}_1(t,S_h(t))}{\mathbb{AB}(\alpha)} +\frac{\alpha\beta}{\mathbb{AB}(\alpha)\Gamma(\alpha)}\int_0^t s^{\beta-1}(t-s)^{\alpha-1}\mathbb{G}_1(s,S_h(s))ds, \tag{4.13}$$

$$(\mathcal{F}_2E_h)(t) = E_h(0)+\frac{\beta t^{\beta-1}(1-\alpha)\mathbb{G}_2(t,E_h(t))}{\mathbb{AB}(\alpha)}$$

$$+\frac{\alpha\beta}{\mathbb{AB}(\alpha)\Gamma(\alpha)}\int_0^t s^{\beta-1}(t-s)^{\alpha-1}\mathbb{G}_2(s,E_h(s))ds, \tag{4.14}$$

$$\begin{aligned}(\mathcal{F}_3 I_h)(t) &= I_h(0)+\frac{\beta t^{\beta-1}(1-\alpha)\mathbb{G}_3(t,I_h(t))}{\mathbb{AB}(\alpha)}\\ &\quad+\frac{\alpha\beta}{\mathbb{AB}(\alpha)\Gamma(\alpha)}\int_0^t s^{\beta-1}(t-s)^{\alpha-1}\mathbb{G}_3(s,I_h(s))ds,\end{aligned} \tag{4.15}$$

$$\begin{aligned}(\mathcal{F}_4 Q_h)(t) &= Q_h(0)+\frac{\beta t^{\beta-1}(1-\alpha)\mathbb{G}_4(t,Q_h(t))}{\mathbb{AB}(\alpha)}\\ &\quad+\frac{\alpha\beta}{\mathbb{AB}(\alpha)\Gamma(\alpha)}\int_0^t s^{\beta-1}(t-s)^{\alpha-1}\mathbb{G}_4(s,Q_h(s))ds,\end{aligned} \tag{4.16}$$

$$\begin{aligned}(\mathcal{F}_5 R_h)(t) &= R_h(0)+\frac{\beta t^{\beta-1}(1-\alpha)\mathbb{G}_5(t,R_h(t))}{\mathbb{AB}(\alpha)}\\ &\quad+\frac{\alpha\beta}{\mathbb{AB}(\alpha)\Gamma(\alpha)}\int_0^t s^{\beta-1}(t-s)^{\alpha-1}\mathbb{G}_5(s,R_h(s))ds,\end{aligned} \tag{4.17}$$

$$\begin{aligned}(\mathcal{F}_6 S_r)(t) &= S_r(0)+\frac{\beta t^{\beta-1}(1-\alpha)\mathbb{G}_6(t,S_r(t))}{\mathbb{AB}(\alpha)}\\ &\quad+\frac{\alpha\beta}{\mathbb{AB}(\alpha)\Gamma(\alpha)}\int_0^t s^{\beta-1}(t-s)^{\alpha-1}\mathbb{G}_6(s,S_r(s))ds,\end{aligned} \tag{4.18}$$

$$\begin{aligned}(\mathcal{F}_7 E_r)(t) &= E_r(0)+\frac{\beta t^{\beta-1}(1-\alpha)\mathbb{G}_7(t,E_r(t))}{\mathbb{AB}(\alpha)}\\ &\quad+\frac{\alpha\beta}{\mathbb{AB}(\alpha)\Gamma(\alpha)}\int_0^t s^{\beta-1}(t-s)^{\alpha-1}\mathbb{G}_7(s,E_r(s))ds,\end{aligned} \tag{4.19}$$

$$\begin{aligned}(\mathcal{F}_8 I_r)(t) &= I_r(0)+\frac{\beta t^{\beta-1}(1-\alpha)\mathbb{G}_8(t,I_r(t))}{\mathbb{AB}(\alpha)}\\ &\quad+\frac{\alpha\beta}{\mathbb{AB}(\alpha)\Gamma(\alpha)}\int_0^t s^{\beta-1}(t-s)^{\alpha-1}\mathbb{G}_8(s,I_r(s))ds.\end{aligned} \tag{4.20}$$

To investigate fixed point theory, we transform the considered model to the fixed point problem $(\mathcal{Y}=\mathcal{T}\mathcal{Y})$, which will apply to create a fixed point theory. Next, we will show that the $\mathbb{FF}$-$\mathbb{MPX}$ model (2.8) has a unique solution.

Theorem 4.2. *Assume that* $\mathbb{G} \in \mathbb{X}$ *satisfies the following assumption*

(A_1) *There exists a constant* $\mathcal{L}_{\max} > 0$, *where* $\mathcal{L}_{\max} = \max\{\mathcal{L}_1, \mathcal{L}_2, \mathcal{L}_3, \mathcal{L}_4, \mathcal{L}_5, \mathcal{L}_6, \mathcal{L}_7, \mathcal{L}_8\}$, *such that*

$$\begin{cases} \big|\mathbb{G}(t, S_h(t), E_h(t), I_h(t), Q_h(t), R_h(t), S_r(t), E_r(t), I_r(t)) \\ \quad -\mathbb{G}(t, S_h^*(t), E_h^*(t), I_h^*(t), Q_h^*(t), R_h^*(t), S_r^*(t), E_r^*(t), I_r^*(t))\big| \\ \leq \mathcal{L}_{\max}\Big(\big|S_h(t) - S_h^*(t)\big| + \big|E_h(t) - E_h^*(t)\big| + \big|I_h(t) - I_h^*(t)\big| + \big|Q_h(t) - Q_h^*(t)\big| \\ \quad + \big|R_h(t) - R_h^*(t)\big| + \big|S_r(t) - S_r^*(t)\big| + \big|E_r(t) - E_r^*(t)\big| + \big|I_r(t) - I_r^*(t)\big|\Big) \end{cases} \tag{4.21}$$

for any S_h, E_h, I_h, R_h, Q_h, S_r, E_r, $I_r \in \mathbb{X}$, *and* $t \in \mathcal{J}$.

If

$$\left(\beta(1-\alpha)T_{\min}^{\beta-1} + \frac{\alpha T^{\alpha+\beta-1}\Gamma(\beta+1)}{\Gamma(\alpha+\beta)}\right)\frac{\mathcal{L}_{\max}}{\mathbb{AB}(\alpha)} < 1, \tag{4.22}$$

then, the $\mathbb{FF}$-$\mathbb{MPX}$ *model* (2.8) *has a unique solution.*

Proof. Now, let D_{r_1} be a bounded, closed, and convex subset, where $D_{r_1} := \Big\{(S_h, E_h, I_h, Q_h, R_h, S_r, E_r, I_r) \in \mathbb{X} : \|(S_h, E_h, I_h, Q_h, R_h, S_r, E_r, I_r)\| \leq r_1\Big\}$ with a radius

$$r_1 \geq \frac{\mathcal{P}_{\max} + \left(\beta(1-\alpha)T_{\min}^{\beta-1} + \frac{\alpha T^{\alpha+\beta-1}\Gamma(\beta+1)}{\Gamma(\alpha+\beta)}\right)\frac{\mathbb{G}_{\max}^*}{\mathbb{AB}(\alpha)}}{1 - \left(\beta(1-\alpha)T_{\min}^{\beta-1} + \frac{\alpha T^{\alpha+\beta-1}\Gamma(\beta+1)}{\Gamma(\alpha+\beta)}\right)\frac{\mathcal{L}_{\max}}{\mathbb{AB}(\alpha)}},$$

where $\mathcal{P}_{\max} = \max\{S_{h_0}, E_{h_0}, I_{h_0}, Q_{h_0}, R_{h_0}, S_{r_0}, E_{r_0}, I_{r_0}\}$, $\mathbb{G}_{\max}^* = \max\{\mathbb{G}_1^*, \mathbb{G}_2^*, \mathbb{G}_3^*, \mathbb{G}_4^*, \mathbb{G}_5^*, \mathbb{G}_6^*, \mathbb{G}_7^*, \mathbb{G}_8^*\}$ and let $\sup_{t\in\mathcal{J}}|\mathbb{G}_i(s,0)| = \mathbb{G}_i^* < +\infty$, for $i = 1, 2, \ldots, 8$.

Step I. We show $\mathcal{F}D_{r_1} \subset D_{r_1}$.

For any $(S_h, E_h, I_h, Q_h, R_h, S_r, E_r, I_r) \in D_{r_1}$, $t \in \mathcal{J}$, we obtain that

$$\begin{aligned} |(\mathcal{T}_1 S_h)(t)| &\leq |S_h(0)| + \frac{\beta t^{\beta-1}(1-\alpha)|\mathbb{G}_1(t, S_h(t))|}{\mathbb{AB}(\alpha)} \\ &\quad + \frac{\alpha\beta}{\mathbb{AB}(\alpha)\Gamma(\alpha)}\int_0^t s^{\beta-1}(t-s)^{\alpha-1}|\mathbb{G}_1(s, S_h(s))|ds \\ &\leq |S_h(0)| + \frac{\beta t^{\beta-1}(1-\alpha)}{\mathbb{AB}(\alpha)}\Big[|\mathbb{G}_1(t, S_h(t)) - \mathbb{G}_1(t,0)| + |\mathbb{G}_1(t,0)|\Big] \\ &\quad + \frac{\alpha\beta}{\mathbb{AB}(\alpha)\Gamma(\alpha)}\int_0^t s^{\beta-1}(t-s)^{\alpha-1}\Big[|\mathbb{G}_1(s, S_h(s)) - \mathbb{G}_1(s,0)| + |\mathbb{G}_1(s,0)|\Big]ds \\ &\leq S_{h_0} + \frac{\beta t^{\beta-1}(1-\alpha)}{\mathbb{AB}(\alpha)}\Big[\mathcal{L}_1\Big(|S_h(t)| + |E_h(t)| + |I_h(t)| + |Q_h(t)| + |R_h(t)| \\ &\quad + |S_r(t)| + |E_r(t)| + |I_r(t)|\Big) + \mathbb{G}_1^*\Big] + \frac{\alpha\beta}{\mathbb{AB}(\alpha)\Gamma(\alpha)}\int_0^t s^{\beta-1}(t-s)^{\alpha-1}\Big[\mathcal{L}_1\Big(|S_h(s)| \\ &\quad + |E_h(s)| + |I_h(s)| + |Q_h(s)| + |R_h(s)| + |S_r(s)| + |E_r(s)| + |I_r(s)|\Big) + \mathbb{G}_1^*\Big]ds \end{aligned}$$

$$\leq S_{h_0}+\left(\frac{\beta(1-\alpha)T_{\min}^{\beta-1}}{\mathbb{AB}(\alpha)}+\frac{\alpha T^{\alpha+\beta-1}\Gamma(\beta+1)}{\mathbb{AB}(\alpha)\Gamma(\alpha+\beta)}\right)\Big[\mathcal{L}_1\Big(\|S_h\|+\|E_h\|+\|I_h\|+\|Q_h\|$$
$$+\|R_h\|+\|S_r\|+\|E_r\|+\|I_r\|\Big)+\mathbb{G}_1^*\Big].$$

This yields that

$$\|\mathcal{T}_1S_h\| \leq S_{h_0}+\left(\frac{\beta(1-\alpha)T_{\min}^{\beta-1}}{\mathbb{AB}(\alpha)}+\frac{\alpha T^{\alpha+\beta-1}\Gamma(\beta+1)}{\mathbb{AB}(\alpha)\Gamma(\alpha+\beta)}\right)\Big[\mathcal{L}_1r_1+\mathbb{G}_1^*\Big]. \tag{4.23}$$

In the same process, it follows that

$$\|\mathcal{T}_2E_h\| \leq E_{h_0}+\left(\frac{\beta(1-\alpha)T_{\min}^{\beta-1}}{\mathbb{AB}(\alpha)}+\frac{\alpha T^{\alpha+\beta-1}\Gamma(\beta+1)}{\mathbb{AB}(\alpha)\Gamma(\alpha+\beta)}\right)\Big[\mathcal{L}_2r_1+\mathbb{G}_2^*\Big], \tag{4.24}$$

$$\|\mathcal{T}_3I_h\| \leq I_{h_0}+\left(\frac{\beta(1-\alpha)T_{\min}^{\beta-1}}{\mathbb{AB}(\alpha)}+\frac{\alpha T^{\alpha+\beta-1}\Gamma(\beta+1)}{\mathbb{AB}(\alpha)\Gamma(\alpha+\beta)}\right)\Big[\mathcal{L}_3r_1+\mathbb{G}_3^*\Big], \tag{4.25}$$

$$\|\mathcal{T}_4Q_h\| \leq Q_{h_0}+\left(\frac{\beta(1-\alpha)T_{\min}^{\beta-1}}{\mathbb{AB}(\alpha)}+\frac{\alpha T^{\alpha+\beta-1}\Gamma(\beta+1)}{\mathbb{AB}(\alpha)\Gamma(\alpha+\beta)}\right)\Big[\mathcal{L}_4r_1+\mathbb{G}_4^*\Big], \tag{4.26}$$

$$\|\mathcal{T}_5R_h\| \leq R_{h_0}+\left(\frac{\beta(1-\alpha)T_{\min}^{\beta-1}}{\mathbb{AB}(\alpha)}+\frac{\alpha T^{\alpha+\beta-1}\Gamma(\beta+1)}{\mathbb{AB}(\alpha)\Gamma(\alpha+\beta)}\right)\Big[\mathcal{L}_5r_1+\mathbb{G}_5^*\Big], \tag{4.27}$$

$$\|\mathcal{T}_6S_r\| \leq S_{r_0}+\left(\frac{\beta(1-\alpha)T_{\min}^{\beta-1}}{\mathbb{AB}(\alpha)}+\frac{\alpha T^{\alpha+\beta-1}\Gamma(\beta+1)}{\mathbb{AB}(\alpha)\Gamma(\alpha+\beta)}\right)\Big[\mathcal{L}_6r_1+\mathbb{G}_6^*\Big], \tag{4.28}$$

$$\|\mathcal{T}_7E_r\| \leq E_{r_0}+\left(\frac{\beta(1-\alpha)T_{\min}^{\beta-1}}{\mathbb{AB}(\alpha)}+\frac{\alpha T^{\alpha+\beta-1}\Gamma(\beta+1)}{\mathbb{AB}(\alpha)\Gamma(\alpha+\beta)}\right)\Big[\mathcal{L}_7r_1+\mathbb{G}_7^*\Big], \tag{4.29}$$

$$\|\mathcal{T}_8I_r\| \leq I_{r_0}+\left(\frac{\beta(1-\alpha)T_{\min}^{\beta-1}}{\mathbb{AB}(\alpha)}+\frac{\alpha T^{\alpha+\beta-1}\Gamma(\beta+1)}{\mathbb{AB}(\alpha)\Gamma(\alpha+\beta)}\right)\Big[\mathcal{L}_8r_1+\mathbb{G}_8^*\Big]. \tag{4.30}$$

From (4.23)–(4.30), implies that $\mathcal{T}D_{r_1}\subset D_{r_1}$.

Step II. We show $\mathcal{T}$ is a contraction.

Assume that $(S_h, E_h, I_h, Q_h, R_h, S_r, E_r, I_r)\in D_{r_1}$ and $(S_h^*, E_h^*, I_h^*, Q_h^*, R_h^*, S_r^*, E_r^*, I_r^*)\in D_{r_1}$, we have

$$\begin{aligned}
&|(\mathcal{T}_1S_h)(t)-(\mathcal{T}_1S_h^*)(t)|\\
\leq\ &\frac{\beta t^{\beta-1}(1-\alpha)}{\mathbb{AB}(\alpha)}|\mathbb{G}_1(t,S_h(t))-\mathbb{G}_1(t,S_h^*(t))|\\
&+\frac{\alpha\beta}{\mathbb{AB}(\alpha)\Gamma(\alpha)}\int_0^t s^{\beta-1}(t-s)^{\alpha-1}|\mathbb{G}_1(s,S_h(s))-\mathbb{G}_1(s,S_h^*(s))|ds\\
\leq\ &\frac{\beta t^{\beta-1}(1-\alpha)}{\mathbb{AB}(\alpha)}\Big[\mathcal{L}_1\Big(|S_h(t)-S_h^*(t)|+|E_h(t)-E_h^*(t)|+|I_h(t)-I_h^*(t)|+|Q_h(t)-Q_h^*(t)|
\end{aligned}$$

$$
\begin{aligned}
&+|R_h(t)-R_h^*(t)|+|S_r(t)-S_r^*(t)|+|E_r(t)-E_r^*(t)|+|I_r(t)-I_r^*(t)|\Big)\Big]\\
&+\frac{\alpha\beta}{\mathbb{AB}(\alpha)\Gamma(\alpha)}\int_0^t s^{\beta-1}(t-s)^{\alpha-1}\Big[\mathcal{L}_1\Big(|S_h(s)-S_h^*(s)|+|E_h(s)-E_h^*(s)|+|I_h(s)-I_h^*(s)|\\
&+|Q_h(s)-Q_h^*(s)|+|R_h(s)-R_h^*(s)|+|S_r(s)-S_r^*(s)|+|E_r(s)-E_r^*(s)|+|I_r(s)-I_r^*(s)|\Big)\Big]ds\\
\leq\ &\left(\beta(1-\alpha)T_{\min}^{\beta-1}+\frac{\alpha T^{\alpha+\beta-1}\Gamma(\beta+1)}{\Gamma(\alpha+\beta)}\right)\frac{\mathcal{L}_1}{\mathbb{AB}(\alpha)}\Big(\|S_h-S_h^*\|+\|E_h-E_h^*\|+\|I_h-I_h^*\|\\
&+\|Q_h-Q_h^*\|+\|R_h-R_h^*\|+\|S_r-S_r^*\|+\|E_r-E_r^*\|+\|I_r-I_r^*\|\Big),
\end{aligned}
$$

then,

$$
\begin{aligned}
\|\mathcal{T}_1S_h-\mathcal{T}_1S_h^*\| \leq\ &\left(\beta(1-\alpha)T_{\min}^{\beta-1}+\frac{\alpha T^{\alpha+\beta-1}\Gamma(\beta+1)}{\Gamma(\alpha+\beta)}\right)\frac{\mathcal{L}_1}{\mathbb{AB}(\alpha)}\Big(\|S_h-S_h^*\|+\|E_h-E_h^*\|+\|I_h-I_h^*\|\\
&+\|Q_h-Q_h^*\|+\|R_h-R_h^*\|+\|S_r-S_r^*\|+\|E_r-E_r^*\|+\|I_r-I_r^*\|\Big). \qquad (4.31)
\end{aligned}
$$

Similarly procedure, which implies that

$$
\begin{aligned}
\|\mathcal{T}_2E_h-\mathcal{T}_2E_h^*\| \leq\ &\left(\beta(1-\alpha)T_{\min}^{\beta-1}+\frac{\alpha T^{\alpha+\beta-1}\Gamma(\beta+1)}{\Gamma(\alpha+\beta)}\right)\frac{\mathcal{L}_2}{\mathbb{AB}(\alpha)}\Big(\|S_h-S_h^*\|+\|E_h-E_h^*\|+\|I_h-I_h^*\|\\
&+\|Q_h-Q_h^*\|+\|R_h-R_h^*\|+\|S_r-S_r^*\|+\|E_r-E_r^*\|+\|I_r-I_r^*\|\Big), \qquad (4.32)\\
\|\mathcal{T}_3I_h-\mathcal{T}_3I_h^*\| \leq\ &\left(\beta(1-\alpha)T_{\min}^{\beta-1}+\frac{\alpha T^{\alpha+\beta-1}\Gamma(\beta+1)}{\Gamma(\alpha+\beta)}\right)\frac{\mathcal{L}_3}{\mathbb{AB}(\alpha)}\Big(\|S_h-S_h^*\|+\|E_h-E_h^*\|+\|I_h-I_h^*\|\\
&+\|Q_h-Q_h^*\|+\|R_h-R_h^*\|+\|S_r-S_r^*\|+\|E_r-E_r^*\|+\|I_r-I_r^*\|\Big), \qquad (4.33)\\
\|\mathcal{T}_4Q_h-\mathcal{T}_4Q_h^*\| \leq\ &\left(\beta(1-\alpha)T_{\min}^{\beta-1}+\frac{\alpha T^{\alpha+\beta-1}\Gamma(\beta+1)}{\Gamma(\alpha+\beta)}\right)\frac{\mathcal{L}_4}{\mathbb{AB}(\alpha)}\Big(\|S_h-S_h^*\|+\|E_h-E_h^*\|+\|I_h-I_h^*\|\\
&+\|Q_h-Q_h^*\|+\|R_h-R_h^*\|+\|S_r-S_r^*\|+\|E_r-E_r^*\|+\|I_r-I_r^*\|\Big), \qquad (4.34)\\
\|\mathcal{T}_5R_h-\mathcal{T}_5R_h^*\| \leq\ &\left(\beta(1-\alpha)T_{\min}^{\beta-1}+\frac{\alpha T^{\alpha+\beta-1}\Gamma(\beta+1)}{\Gamma(\alpha+\beta)}\right)\frac{\mathcal{L}_5}{\mathbb{AB}(\alpha)}\Big(\|S_h-S_h^*\|+\|E_h-E_h^*\|+\|I_h-I_h^*\|\\
&+\|Q_h-Q_h^*\|+\|R_h-R_h^*\|+\|S_r-S_r^*\|+\|E_r-E_r^*\|+\|I_r-I_r^*\|\Big), \qquad (4.35)\\
\|\mathcal{T}_6S_r-\mathcal{T}_6S_r^*\| \leq\ &\left(\beta(1-\alpha)T_{\min}^{\beta-1}+\frac{\alpha T^{\alpha+\beta-1}\Gamma(\beta+1)}{\Gamma(\alpha+\beta)}\right)\frac{\mathcal{L}_6}{\mathbb{AB}(\alpha)}\Big(\|S_h-S_h^*\|+\|E_h-E_h^*\|+\|I_h-I_h^*\|\\
&+\|Q_h-Q_h^*\|+\|R_h-R_h^*\|+\|S_r-S_r^*\|+\|E_r-E_r^*\|+\|I_r-I_r^*\|\Big), \qquad (4.36)\\
\|\mathcal{T}_7E_r-\mathcal{T}_7E_r^*\| \leq\ &\left(\beta(1-\alpha)T_{\min}^{\beta-1}+\frac{\alpha T^{\alpha+\beta-1}\Gamma(\beta+1)}{\Gamma(\alpha+\beta)}\right)\frac{\mathcal{L}_7}{\mathbb{AB}(\alpha)}\Big(\|S_h-S_h^*\|+\|E_h-E_h^*\|+\|I_h-I_h^*\|\\
&+\|Q_h-Q_h^*\|+\|R_h-R_h^*\|+\|S_r-S_r^*\|+\|E_r-E_r^*\|+\|I_r-I_r^*\|\Big), \qquad (4.37)
\end{aligned}
$$

$$\begin{aligned}\|\mathcal{T}_8 I_r - \mathcal{T}_8 I_r^*\| \;\leq\; & \left(\beta(1-\alpha)T_{\min}^{\beta-1} + \frac{\alpha T^{\alpha+\beta-1}\Gamma(\beta+1)}{\Gamma(\alpha+\beta)}\right)\frac{\mathcal{L}_8}{\mathbb{AB}(\alpha)}\Big(\|S_h - S_h^*\| + \|E_h - E_h^*\| + \|I_h - I_h^*\| \\ & + \|Q_h - Q_h^*\| + \|R_h - R_h^*\| + \|S_r - S_r^*\| + \|E_r - E_r^*\| + \|I_r - I_r^*\|\Big). \end{aligned} \tag{4.38}$$

Since, $\mathcal{T} = (\mathcal{T}_1, \mathcal{T}_2, \mathcal{T}_3, \mathcal{T}_4, \mathcal{T}_5, \mathcal{T}_6, \mathcal{T}_7, \mathcal{T}_8)$ and $\mathcal{L}_{\max} > 0$ with the results (4.31)–(4.38), we obtain

$$\begin{aligned} & \|\mathcal{T}(S_h, E_h, I_h, Q_h, R_h, S_r, E_r, I_r) - \mathcal{T}(S_h^*, E_h^*, I_h^*, Q_h^*, R_h^*, S_r^*, E_r^*, I_r^*)\| \\ \leq\; & \left(\beta(1-\alpha)T_{\min}^{\beta-1} + \frac{\alpha T^{\alpha+\beta-1}\Gamma(\beta+1)}{\Gamma(\alpha+\beta)}\right)\frac{\mathcal{L}_{\max}}{\mathbb{AB}(\alpha)}\Big(\|S_h - S_h^*\| + \|E_h - E_h^*\| \\ & + \|I_h - I_h^*\| + \|Q_h - Q_h^*\| + \|R_h - R_h^*\| + \|S_r - S_r^*\| + \|E_r - E_r^*\| + \|I_r - I_r^*\|\Big). \end{aligned}$$

By the condition (4.22), then, $\mathcal{T}$ is a contraction. Therefore, by Lemma 2.5, the $\mathbb{FF}$-$\mathbb{MPX}$ model (2.8) has a solution. □

Theorem 4.3. *Assume that* $\mathbb{G} \in \mathbb{X}$ *satisfies the assumptions* (A_1) *in Theorem 4.2, and*

(A_2) *There exist constants* $g_{ij} > 0$, $i = 0, 1, \ldots, 8$, $j = 1, 2, \ldots, 8$, *such that*

$$\begin{cases} \left|\mathbb{G}(t, S_h(t), E_h(t), I_h(t), R_h(t), Q_h(t), S_r(t), E_r(t), I_r(t))\right| \\ \quad \leq g_{0j} + g_{1j}\left|S_h(t)\right| + g_{2j}\left|E_h(t)\right| + g_{3j}\left|I_h(t)\right| + g_{4j}\left|R_h(t)\right| \\ \quad\quad + g_{5j}\left|\mathbb{Q}_h(t)\right| + g_{6j}\left|S_r(t)\right| + g_{7j}\left|E_r(t)\right| + g_{8j}\left|I_r(t)\right|. \end{cases} \tag{4.39}$$

If

$$\beta(1-\alpha)T_{\min}^{\beta-1}\mathcal{L}_{\max} < \mathbb{AB}(\alpha), \tag{4.40}$$

then, the $\mathbb{FF}$-$\mathbb{MPX}$ *model* (2.8) *has at least one solution.*

Proof. Define a set $D_{r_2} := \{(S_h, E_h, I_h, Q_h, R_h, S_r, E_r, I_r) \in \mathbb{X} : \|(S_h, E_h, I_h, Q_h, R_h, S_r, E_r, I_r)\| \leq r_2\}$.

By applying (4.5)–(4.12), we can be defined two operators $\mathcal{Q}, \mathcal{P} : D_{r_2} \to \mathbb{X}$ where $\mathcal{Q} = (\mathcal{Q}_1, \mathcal{Q}_2, \mathcal{Q}_3, \mathcal{Q}_4, \mathcal{Q}_5, \mathcal{Q}_6, \mathcal{Q}_7, \mathcal{Q}_8)$ and $\mathcal{P} = (\mathcal{P}_1, \mathcal{P}_2, \mathcal{P}_3, \mathcal{P}_4, \mathcal{P}_5, \mathcal{P}_6, \mathcal{P}_7, \mathcal{P}_8)$. The operator $\mathcal{Q}$ is defined by

$$\begin{cases} (Q_1S_h)(t) = S_h(0) + \dfrac{\beta t^{\beta-1}(1-\alpha)\mathbb{G}_1(t,S_h(t))}{\mathbb{AB}(\alpha)}, \\ (Q_2E_h)(t) = E_h(0) + \dfrac{\beta t^{\beta-1}(1-\alpha)\mathbb{G}_2(t,E_h(t))}{\mathbb{AB}(\alpha)}, \\ (Q_3I_h)(t) = I_h(0) + \dfrac{\beta t^{\beta-1}(1-\alpha)\mathbb{G}_3(t,I_h(t))}{\mathbb{AB}(\alpha)}, \\ (Q_4Q_h)(t) = Q_h(0) + \dfrac{\beta t^{\beta-1}(1-\alpha)\mathbb{G}_4(t,Q_h(t))}{\mathbb{AB}(\alpha)}, \\ (Q_5R_h)(t) = R_h(0) + \dfrac{\beta t^{\beta-1}(1-\alpha)\mathbb{G}_5(t,R_h(t))}{\mathbb{AB}(\alpha)}, \\ (Q_6S_r)(t) = S_r(0) + \dfrac{\beta t^{\beta-1}(1-\alpha)\mathbb{G}_6(t,S_r(t))}{\mathbb{AB}(\alpha)}, \\ (Q_7E_r)(t) = E_r(0) + \dfrac{\beta t^{\beta-1}(1-\alpha)\mathbb{G}_7(t,E_r(t))}{\mathbb{AB}(\alpha)}, \\ (Q_8I_r)(t) = I_r(0) + \dfrac{\beta t^{\beta-1}(1-\alpha)\mathbb{G}_8(t,I_r(t))}{\mathbb{AB}(\alpha)}, \end{cases} \tag{4.41}$$

and the operator $\mathcal{P}$ is defined by

$$\begin{cases} (\mathcal{P}_1S_h)(t) = \dfrac{\alpha\beta}{\mathbb{AB}(\alpha)\Gamma(\alpha)}\displaystyle\int_0^t s^{\beta-1}(t-s)^{\alpha-1}\mathbb{G}_1(s,S_h(s))ds, \\ (\mathcal{P}_2E_h)(t) = \dfrac{\alpha\beta}{\mathbb{AB}(\alpha)\Gamma(\alpha)}\displaystyle\int_0^t s^{\beta-1}(t-s)^{\alpha-1}\mathbb{G}_2(s,E_h(s))ds, \\ (\mathcal{P}_3I_h)(t) = \dfrac{\alpha\beta}{\mathbb{AB}(\alpha)\Gamma(\alpha)}\displaystyle\int_0^t s^{\beta-1}(t-s)^{\alpha-1}\mathbb{G}_3(s,I_h(s))ds, \\ (\mathcal{P}_4Q_h)(t) = \dfrac{\alpha\beta}{\mathbb{AB}(\alpha)\Gamma(\alpha)}\displaystyle\int_0^t s^{\beta-1}(t-s)^{\alpha-1}\mathbb{G}_4(s,Q_h(s))ds, \\ (\mathcal{P}_5R_h)(t) = \dfrac{\alpha\beta}{\mathbb{AB}(\alpha)\Gamma(\alpha)}\displaystyle\int_0^t s^{\beta-1}(t-s)^{\alpha-1}\mathbb{G}_5(s,R_h(s))ds, \\ (\mathcal{P}_6S_r)(t) = \dfrac{\alpha\beta}{\mathbb{AB}(\alpha)\Gamma(\alpha)}\displaystyle\int_0^t s^{\beta-1}(t-s)^{\alpha-1}\mathbb{G}_6(s,S_r(s))ds, \\ (\mathcal{P}_7E_r)(t) = \dfrac{\alpha\beta}{\mathbb{AB}(\alpha)\Gamma(\alpha)}\displaystyle\int_0^t s^{\beta-1}(t-s)^{\alpha-1}\mathbb{G}_7(s,E_r(s))ds, \\ (\mathcal{P}_8I_r)(t) = \dfrac{\alpha\beta}{\mathbb{AB}(\alpha)\Gamma(\alpha)}\displaystyle\int_0^t s^{\beta-1}(t-s)^{\alpha-1}\mathbb{G}_8(s,I_r(s))ds. \end{cases} \tag{4.42}$$

Using (A_1) in Theorem 4.2, for any $(S_h, E_h, I_h, Q_h, R_h, S_r, E_r, I_r) \in D_{r_1}$ and $(S_h^*, E_h^*, I_h^*, Q_h^*, R_h^*, S_r^*, E_r^*, I_r^*) \in D_{r_1}$, we have

$$\begin{aligned} \|Q_1S_h - Q_1S_h^*\| &\leq \frac{\beta(1-\alpha)T_{\min}^{\beta-1}}{\mathbb{AB}(\alpha)}\sup_{t\in\mathcal{J}}\left|\mathbb{G}_1(t,S_h(t)) - \mathbb{G}_1(t,S_h^*(t))\right| \\ &\leq \frac{\beta(1-\alpha)T_{\min}^{\beta-1}\mathcal{L}_1}{\mathbb{AB}(\alpha)}\Big(\|S_h - S_h^*\| + \|E_h - E_h^*\| + \|I_h - I_h^*\| + \|Q_h - Q_h^*\| \end{aligned}$$

$$+\|R_h - R_h^*\| + \|S_r - S_r^*\| + \|E_r - E_r^*\| + \|I_r - I_r^*\|\Big). \tag{4.43}$$

In the same process, we obtain that the following results

$$\begin{aligned}
\|Q_2E_h - Q_2E_h^*\| &\leq \frac{\beta(1-\alpha)T_{\min}^{\beta-1}\mathcal{L}_2}{\mathbb{AB}(\alpha)}\Big(\|S_h - S_h^*\| + \|E_h - E_h^*\| + \|I_h - I_h^*\| + \|Q_h - Q_h^*\| \\
&\quad +\|R_h - R_h^*\| + \|S_r - S_r^*\| + \|E_r - E_r^*\| + \|I_r - I_r^*\|\Big), \qquad (4.44)\\
\|Q_3I_h - Q_3I_h^*\| &\leq \frac{\beta(1-\alpha)T_{\min}^{\beta-1}\mathcal{L}_3}{\mathbb{AB}(\alpha)}\Big(\|S_h - S_h^*\| + \|E_h - E_h^*\| + \|I_h - I_h^*\| + \|Q_h - Q_h^*\| \\
&\quad +\|R_h - R_h^*\| + \|S_r - S_r^*\| + \|E_r - E_r^*\| + \|I_r - I_r^*\|\Big), \qquad (4.45)\\
\|Q_4Q_h - Q_4Q_h^*\| &\leq \frac{\beta(1-\alpha)T_{\min}^{\beta-1}\mathcal{L}_4}{\mathbb{AB}(\alpha)}\Big(\|S_h - S_h^*\| + \|E_h - E_h^*\| + \|I_h - I_h^*\| + \|Q_h - Q_h^*\| \\
&\quad +\|R_h - R_h^*\| + \|S_r - S_r^*\| + \|E_r - E_r^*\| + \|I_r - I_r^*\|\Big), \qquad (4.46)\\
\|Q_5R_h - Q_5R_h^*\| &\leq \frac{\beta(1-\alpha)T_{\min}^{\beta-1}\mathcal{L}_5}{\mathbb{AB}(\alpha)}\Big(\|S_h - S_h^*\| + \|E_h - E_h^*\| + \|I_h - I_h^*\| + \|Q_h - Q_h^*\| \\
&\quad +\|R_h - R_h^*\| + \|S_r - S_r^*\| + \|E_r - E_r^*\| + \|I_r - I_r^*\|\Big), \qquad (4.47)\\
\|Q_6S_r - Q_6S_r^*\| &\leq \frac{\beta(1-\alpha)T_{\min}^{\beta-1}\mathcal{L}_6}{\mathbb{AB}(\alpha)}\Big(\|S_h - S_h^*\| + \|E_h - E_h^*\| + \|I_h - I_h^*\| + \|Q_h - Q_h^*\| \\
&\quad +\|R_h - R_h^*\| + \|S_r - S_r^*\| + \|E_r - E_r^*\| + \|I_r - I_r^*\|\Big), \qquad (4.48)\\
\|Q_7E_r - Q_7E_r^*\| &\leq \frac{\beta(1-\alpha)T_{\min}^{\beta-1}\mathcal{L}_7}{\mathbb{AB}(\alpha)}\Big(\|S_h - S_h^*\| + \|E_h - E_h^*\| + \|I_h - I_h^*\| + \|Q_h - Q_h^*\| \\
&\quad +\|R_h - R_h^*\| + \|S_r - S_r^*\| + \|E_r - E_r^*\| + \|I_r - I_r^*\|\Big), \qquad (4.49)\\
\|Q_8I_r - Q_8I_r^*\| &\leq \frac{\beta(1-\alpha)T_{\min}^{\beta-1}\mathcal{L}_8}{\mathbb{AB}(\alpha)}\Big(\|S_h - S_h^*\| + \|E_h - E_h^*\| + \|I_h - I_h^*\| + \|Q_h - Q_h^*\| \\
&\quad +\|R_h - R_h^*\| + \|S_r - S_r^*\| + \|E_r - E_r^*\| + \|I_r - I_r^*\|\Big). \qquad (4.50)
\end{aligned}$$

From (4.43)–(4.50) with $\mathcal{L}_{\max}$, it follows that

$$\begin{aligned}
&\Big\|\mathcal{Q}(S_h, E_h, I_h, Q_h, R_h, S_r, E_r, I_r) - \mathcal{Q}(S_h^*, E_h^*, I_h^*, Q_h^*, R_h^*, S_r^*, E_r^*, I_r^*)\Big\| \\
&\leq \frac{\beta(1-\alpha)T_{\min}^{\beta-1}\mathcal{L}_{\max}}{\mathbb{AB}(\alpha)}\Big\|(S_h, E_h, I_h, Q_h, R_h, S_r, E_r, I_r) - (S_h^*, E_h^*, I_h^*, Q_h^*, R_h^*, S_r^*, E_r^*, I_r^*)\Big\|.
\end{aligned}$$

Therefore, $\mathcal{Q}$ is a contraction.

Next, we prove that $\mathcal{P}$ is continuous and compact, which yields that $\mathcal{P}$ is completely continuous. Then, it is sufficient condition to prove that $\mathcal{P}$ is bounded and equicontinuous. Using (A_2), it is

obviously that $\mathcal{P}$ is continuous as Q is also continuous. Hence, for any $t \in \mathcal{J}$, we get

$$\begin{aligned}
\|\mathcal{P}_1 S_h\| &\leq \frac{\alpha\beta}{\mathbb{AB}(\alpha)\Gamma(\alpha)} \sup_{t\in\mathcal{J}} \left| \int_0^t s^{\beta-1}(t-s)^{\alpha-1}\mathbb{G}_1(s, S_h(s))ds \right| \\
&\leq \frac{\alpha\beta}{\mathbb{AB}(\alpha)\Gamma(\alpha)} \int_0^t s^{\beta-1}(t-s)^{\alpha-1} \sup_{t\in\mathcal{J}} \left|\mathbb{G}_1(s, S_h(s))\right| ds \\
&\leq \frac{\alpha T^{\alpha+\beta-1}\Gamma(\beta+1)}{\mathbb{AB}(\alpha)\Gamma(\alpha+\beta)} \Big[g_{01} + g_{11}\|S_h\| + g_{21}\|E_h\| + g_{31}\|I_h\| + g_{41}\|R_h\| \\
&\quad + g_{51}\|Q_h\| + g_{61}\|S_r\| + g_{71}\|E_r\| + g_{81}\|I_r\| \Big]. \qquad (4.51)
\end{aligned}$$

Then, $\mathcal{P}_1$ is bounded. In the same ways, we have

$$\begin{aligned}
\|\mathcal{P}_2 E_h\| &\leq \frac{\alpha T^{\alpha+\beta-1}\Gamma(\beta+1)}{\mathbb{AB}(\alpha)\Gamma(\alpha+\beta)} \Big[g_{02} + g_{12}\|S_h\| + g_{22}\|E_h\| + g_{32}\|I_h\| + g_{42}\|R_h\| \\
&\quad + g_{52}\|Q_h\| + g_{62}\|S_r\| + g_{72}\|E_r\| + g_{82}\|I_r\| \Big], \qquad (4.52) \\
\|\mathcal{P}_3 I_h\| &\leq \frac{\alpha T^{\alpha+\beta-1}\Gamma(\beta+1)}{\mathbb{AB}(\alpha)\Gamma(\alpha+\beta)} \Big[g_{03} + g_{13}\|S_h\| + g_{23}\|E_h\| + g_{33}\|I_h\| + g_{43}\|R_h\| \\
&\quad + g_{53}\|Q_h\| + g_{63}\|S_r\| + g_{73}\|E_r\| + g_{83}\|I_r\| \Big], \qquad (4.53) \\
\|\mathcal{P}_4 Q_h\| &\leq \frac{\alpha T^{\alpha+\beta-1}\Gamma(\beta+1)}{\mathbb{AB}(\alpha)\Gamma(\alpha+\beta)} \Big[g_{04} + g_{14}\|S_h\| + g_{24}\|E_h\| + g_{34}\|I_h\| + g_{44}\|R_h\| \\
&\quad + g_{54}\|Q_h\| + g_{64}\|S_r\| + g_{74}\|E_r\| + g_{84}\|I_r\| \Big], \qquad (4.54) \\
\|\mathcal{P}_5 R_h\| &\leq \frac{\alpha T^{\alpha+\beta-1}\Gamma(\beta+1)}{\mathbb{AB}(\alpha)\Gamma(\alpha+\beta)} \Big[g_{05} + g_{15}\|S_h\| + g_{25}\|E_h\| + g_{35}\|I_h\| + g_{45}\|R_h\| \\
&\quad + g_{55}\|Q_h\| + g_{65}\|S_r\| + g_{75}\|E_r\| + g_{85}\|I_r\| \Big], \qquad (4.55) \\
\|\mathcal{P}_6 S_r\| &\leq \frac{\alpha T^{\alpha+\beta-1}\Gamma(\beta+1)}{\mathbb{AB}(\alpha)\Gamma(\alpha+\beta)} \Big[g_{06} + g_{16}\|S_h\| + g_{26}\|E_h\| + g_{36}\|I_h\| + g_{46}\|R_h\| \\
&\quad + g_{56}\|Q_h\| + g_{66}\|S_r\| + g_{76}\|E_r\| + g_{86}\|I_r\| \Big], \qquad (4.56) \\
\|\mathcal{P}_7 E_r\| &\leq \frac{\alpha T^{\alpha+\beta-1}\Gamma(\beta+1)}{\mathbb{AB}(\alpha)\Gamma(\alpha+\beta)} \Big[g_{07} + g_{17}\|S_h\| + g_{27}\|E_h\| + g_{37}\|I_h\| + g_{47}\|R_h\| \\
&\quad + g_{57}\|Q_h\| + g_{67}\|S_r\| + g_{77}\|E_r\| + g_{87}\|I_r\| \Big], \qquad (4.57) \\
\|\mathcal{P}_8 I_r\| &\leq \frac{\alpha T^{\alpha+\beta-1}\Gamma(\beta+1)}{\mathbb{AB}(\alpha)\Gamma(\alpha+\beta)} \Big[g_{08} + g_{18}\|S_h\| + g_{28}\|E_h\| + g_{38}\|I_h\| + g_{48}\|R_h\| \\
&\quad + g_{58}\|Q_h\| + g_{68}\|S_r\| + g_{78}\|E_r\| + g_{88}\|I_r\| \Big]. \qquad (4.58)
\end{aligned}$$

By applying (4.51)–(4.58) and setting $\|\mathcal{P}\| = \max\{\|\mathcal{P}_1\| + \|\mathcal{P}_2\| + \|\mathcal{P}_3\| + \|\mathcal{P}_4\| + \|\mathcal{P}_5\| + \|\mathcal{P}_6\| + \|\mathcal{P}_7\| + \|\mathcal{P}_8\|\}$ with $g_0^* = \max\{g_{0j}\}$, $g_1^* = \max\{g_{1j}\}$, $g_2^* = \max\{g_{2j}\}$, $g_3^* = \max\{g_{3j}\}$, $g_4^* = \max\{g_{4j}\}$,

$g_5^* = \max\{g_{5j}\}$, $g_6^* = \max\{g_{6j}\}$, $g_7^* = \max\{g_{7j}\}$, and $g_8^* = \max\{g_{8j}\}$ for $j = 1, 2, \ldots, 8$, it follows that

$$\begin{aligned}\left\|\mathcal{P}(S_h, E_h, I_h, Q_h, R_h, S_r, E_r, I_r)\right\| \leq\ & \frac{\alpha T^{\alpha+\beta-1}\Gamma(\beta+1)}{\mathbb{AB}(\alpha)\Gamma(\alpha+\beta)}\Big[g_0^* + g_1^*\|S_h\| + g_2^*\|E_h\| + g_3^*\|I_h\| + g_4^*\|R_h\| \\ & + g_5^*\|Q_h\| + g_6^*\|S_r\| + g_7^*\|E_r\| + g_8^*\|I_r\|\Big].\end{aligned}$$

This implies that $\mathcal{P}$ is bounded. Next, we prove that $\mathcal{P}$ is equicontinuity. Suppose that t_1, $t_2 \in \mathcal{J}$ with $0 \leq t_1 < t_2 \leq T$, we obtain that

$$\begin{aligned}& \left|(\mathcal{P}_1 S_h)(t_2) - (\mathcal{P}_1 S_h)(t_1)\right| \\ \leq\ & \frac{\alpha\beta}{\mathbb{AB}(\alpha)\Gamma(\alpha)}\left|\int_0^{t_2} s^{\beta-1}(t_2 - s)^{\alpha-1}ds - \int_0^{t_1} s^{\beta-1}(t_1 - s)^{\alpha-1}ds\right||\mathbb{G}_1(s, S_h(s))| \\ \leq\ & \frac{\alpha\Gamma(\beta+1)}{\mathbb{AB}(\alpha)\Gamma(\alpha+\beta)}\left|t_1^{\alpha+\beta-1} - t_2^{\alpha+\beta-1} + 2(t_2 - t_1)^{\alpha+\beta-1}\right|\Big[g_{01} + g_{11}\|S_h\| + g_{21}\|E_h\| \\ & + g_{31}\|I_h\| + g_{41}\|R_h\| + g_{51}\|Q_h\| + g_{61}\|S_r\| + g_{71}\|E_r\| + g_{81}\|I_r\|\Big] \\ \leq\ & \frac{\alpha\Gamma(\beta+1)}{\mathbb{AB}(\alpha)\Gamma(\alpha+\beta)}\left|t_1^{\alpha+\beta-1} - t_2^{\alpha+\beta-1} + 2(t_2 - t_1)^{\alpha+\beta-1}\right|\Big[g_{01} + r_2\sum_{i=1}^{8} g_{i1}\Big]. \qquad (4.59)\end{aligned}$$

Notice that, the right side of (4.59) is independent of $(S_h, E_h, I_h, Q_h, R_h, S_r, E_r, I_r)$ and $\left|(\mathcal{P}_1 S_h)(t_2) - (\mathcal{P}_1 S_h)(t_1)\right| \to 0$ as $t_2 \to t_1$, which implies that $\mathcal{P}_1$ is bounded, uniformly continuous and compact that is $\mathcal{P}_1$ is completely continuous.

In the same ways, we have the following inequality

$$\begin{aligned}& \left|(\mathcal{P}_2 E_h)(t_2) - (\mathcal{P}_2 E_h)(t_1)\right| \\ \leq\ & \frac{\alpha\Gamma(\beta+1)}{\mathbb{AB}(\alpha)\Gamma(\alpha+\beta)}\left|t_1^{\alpha+\beta-1} - t_2^{\alpha+\beta-1} + 2(t_2 - t_1)^{\alpha+\beta-1}\right|\Big[g_{02} + r_2\sum_{i=1}^{8} g_{i2}\Big], \qquad (4.60) \\ & \left|(\mathcal{P}_3 I_h)(t_2) - (\mathcal{P}_3 I_h)(t_1)\right| \\ \leq\ & \frac{\alpha\Gamma(\beta+1)}{\mathbb{AB}(\alpha)\Gamma(\alpha+\beta)}\left|t_1^{\alpha+\beta-1} - t_2^{\alpha+\beta-1} + 2(t_2 - t_1)^{\alpha+\beta-1}\right|\Big[g_{03} + r_2\sum_{i=1}^{8} g_{i3}\Big], \qquad (4.61) \\ & \left|(\mathcal{P}_4 Q_h)(t_2) - (\mathcal{P}_4 Q_h)(t_1)\right| \\ \leq\ & \frac{\alpha\Gamma(\beta+1)}{\mathbb{AB}(\alpha)\Gamma(\alpha+\beta)}\left|t_1^{\alpha+\beta-1} - t_2^{\alpha+\beta-1} + 2(t_2 - t_1)^{\alpha+\beta-1}\right|\Big[g_{04} + r_2\sum_{i=1}^{8} g_{i4}\Big], \qquad (4.62) \\ & \left|(\mathcal{P}_5 R_h)(t_2) - (\mathcal{P}_5 R_h)(t_1)\right| \\ \leq\ & \frac{\alpha\Gamma(\beta+1)}{\mathbb{AB}(\alpha)\Gamma(\alpha+\beta)}\left|t_1^{\alpha+\beta-1} - t_2^{\alpha+\beta-1} + 2(t_2 - t_1)^{\alpha+\beta-1}\right|\Big[g_{05} + r_2\sum_{i=1}^{8} g_{i5}\Big], \qquad (4.63) \\ & \left|(\mathcal{P}_6 S_r)(t_2) - (\mathcal{P}_6 S_r)(t_1)\right| \\ \leq\ & \frac{\alpha\Gamma(\beta+1)}{\mathbb{AB}(\alpha)\Gamma(\alpha+\beta)}\left|t_1^{\alpha+\beta-1} - t_2^{\alpha+\beta-1} + 2(t_2 - t_1)^{\alpha+\beta-1}\right|\Big[g_{06} + r_2\sum_{i=1}^{8} g_{i6}\Big], \qquad (4.64)\end{aligned}$$

$$
\begin{aligned}
&\left|(\mathcal{P}_7E_r)(t_2)-(\mathcal{P}_7E_r)(t_1)\right| \\
\leq\ & \frac{\alpha\Gamma(\beta+1)}{\mathbb{AB}(\alpha)\Gamma(\alpha+\beta)}\left|t_1^{\alpha+\beta-1}-t_2^{\alpha+\beta-1}+2(t_2-t_1)^{\alpha+\beta-1}\right|\left[g_{07}+r_2\sum_{i=1}^{8}g_{i7}\right], \qquad (4.65)\\
&\left|(\mathcal{P}_8I_r)(t_2)-(\mathcal{P}_8I_r)(t_1)\right| \\
\leq\ & \frac{\alpha\Gamma(\beta+1)}{\mathbb{AB}(\alpha)\Gamma(\alpha+\beta)}\left|t_1^{\alpha+\beta-1}-t_2^{\alpha+\beta-1}+2(t_2-t_1)^{\alpha+\beta-1}\right|\left[g_{08}+r_2\sum_{i=1}^{8}g_{i8}\right]. \qquad (4.66)
\end{aligned}
$$

Similarly, the above inequality (4.60)–(4.66), that is

$$
\left|\mathcal{P}_i(S_h,E_h,I_h,Q_h,R_h,S_r,E_r,I_r)(t_2)-\mathcal{P}_i(S_h,E_h,I_h,Q_h,R_h,S_r,E_r,I_r)(t_1)\right|\to 0 \text{ as } t_2\to t_1,
$$

for $i=2,3,\ldots,8$, this yields that $\mathcal{P}_i$, $i=2,3,\ldots,8$, is bounded, uniformly continuous and compact. This means $\mathcal{P}_i$ is completely continuous, for $i=2,3,\ldots,8$.

By utilizing (4.59)–(4.66) and taking $\|\mathcal{P}\|$ with g_j^* for $j=0,1,\ldots,8$, we have

$$
\begin{aligned}
&\left|\mathcal{P}(S_h,E_h,I_h,Q_h,R_h,S_r,E_r,I_r)(t_2)-\mathcal{P}(S_h,E_h,I_h,Q_h,R_h,S_r,E_r,I_r)(t_1)\right| \\
\leq\ & \frac{\alpha\Gamma(\beta+1)}{\mathbb{AB}(\alpha)\Gamma(\alpha+\beta)}\left|t_1^{\alpha+\beta-1}-t_2^{\alpha+\beta-1}+2(t_2-t_1)^{\alpha+\beta-1}\right|\left[g_0^*+r_2\sum_{i=1}^{8}g_i^*\right]. \qquad (4.67)
\end{aligned}
$$

Then, $\mathcal{P}$ is bounded, uniformly continuous and compact that is $\mathcal{P}$ is completely continuous. Therefore, by Lemma 2.6, the $\mathbb{FF}$-$\mathbb{MPX}$ model (2.8) has at least one solution. □

5. Numerical schemes for the $\mathbb{FF}$-$\mathbb{MPX}$ model

This section uses the Adams-Bashforth method based on two steps of Lagrange polynomials to generate the numerical schemes for the $\mathbb{FF}$-$\mathbb{MPX}$ model (2.8). We re-write these integral equations (4.5)–(4.12) at $t=t_{n+1}$, this yields

$$
\begin{aligned}
S_h(t_{n+1}) &= S_{h_0}+\frac{\beta(1-\alpha)t_n^{\beta-1}\mathbb{G}_1(t_n,S_h(t_n))}{\mathbb{AB}(\alpha)}+\frac{\alpha\beta}{\mathbb{AB}(\alpha)\Gamma(\alpha)}\int_0^{t_{n+1}}(t_{n+1}-s)^{\alpha-1}s^{\beta-1}\mathbb{G}_1(s,S_h(s))ds,\\
E_h(t_{n+1}) &= E_{h_0}+\frac{\beta(1-\alpha)t_n^{\beta-1}\mathbb{G}_2(t_n,E_h(t_n))}{\mathbb{AB}(\alpha)}+\frac{\alpha\beta}{\mathbb{AB}(\alpha)\Gamma(\alpha)}\int_0^{t_{n+1}}(t_{n+1}-s)^{\alpha-1}s^{\beta-1}\mathbb{G}_2(s,E_h(s))ds,\\
I_h(t_{n+1}) &= I_{h_0}+\frac{\beta(1-\alpha)t_n^{\beta-1}\mathbb{G}_3(t_n,I_h(t_n))}{\mathbb{AB}(\alpha)}+\frac{\alpha\beta}{\mathbb{AB}(\alpha)\Gamma(\alpha)}\int_0^{t_{n+1}}(t_{n+1}-s)^{\alpha-1}s^{\beta-1}\mathbb{G}_3(s,I_h(s))ds,\\
Q_h(t_{n+1}) &= Q_{h_0}+\frac{\beta(1-\alpha)t_n^{\beta-1}\mathbb{G}_4(\xi_n,Q_h(t_n))}{\mathbb{AB}(\alpha)}+\frac{\alpha\beta}{\mathbb{AB}(\alpha)\Gamma(\alpha)}\int_0^{t_{n+1}}(t_{n+1}-s)^{\alpha-1}s^{\beta-1}\mathbb{G}_4(s,Q_h(s))ds,\\
R_h(t_{n+1}) &= R_{h_0}+\frac{\beta(1-\alpha)t_n^{\beta-1}\mathbb{G}_5(t_n,R_h(t_n))}{\mathbb{AB}(\alpha)}+\frac{\alpha\beta}{\mathbb{AB}(\alpha)\Gamma(\alpha)}\int_0^{t_{n+1}}(t_{n+1}-s)^{\alpha-1}s^{\beta-1}\mathbb{G}_5(s,R_h(s))ds,\\
S_r(t_{n+1}) &= S_{r_0}+\frac{\beta(1-\alpha)t_n^{\beta-1}\mathbb{G}_6(t_n,S_r(t_n))}{\mathbb{AB}(\alpha)}+\frac{\alpha\beta}{\mathbb{AB}(\alpha)\Gamma(\alpha)}\int_0^{t_{n+1}}(t_{n+1}-s)^{\alpha-1}s^{\beta-1}\mathbb{G}_6(s,S_r(s))ds,
\end{aligned}
$$

$$E_r(t_{n+1}) = E_{r_0} + \frac{\beta(1-\alpha)t_n^{\beta-1}\mathbb{G}_7(t_n, E_r(t_n))}{\mathbb{AB}(\alpha)} + \frac{\alpha\beta}{\mathbb{AB}(\alpha)\Gamma(\alpha)}\int_0^{t_{n+1}}(t_{n+1}-s)^{\alpha-1}s^{\beta-1}\mathbb{G}_7(s, E_r(s))ds,$$

$$I_r(t_{n+1}) = I_{r_0} + \frac{\beta(1-\alpha)t_n^{\beta-1}\mathbb{G}_8(t_n, I_r(t_n))}{\mathbb{AB}(\alpha)} + \frac{\alpha\beta}{\mathbb{AB}(\alpha)\Gamma(\alpha)}\int_0^{t_{n+1}}(t_{n+1}-s)^{\alpha-1}s^{\beta-1}\mathbb{G}_8(s, I_r(s))ds.$$

So, the numerical approximation of the above integrals is formulated by

$$\begin{aligned}
S_h(t_{n+1}) &= S_{h_0} + \frac{\beta(1-\alpha)t_n^{\beta-1}\mathbb{G}_1(t_n, S_h(t_n))}{\mathbb{AB}(\alpha)} \\
&\quad + \frac{\alpha\beta}{\mathbb{AB}(\alpha)\Gamma(\alpha)}\sum_{j=1}^{n}\int_{t_j}^{t_{j+1}}(t_{j+1}-s)^{\alpha-1}s^{\beta-1}\mathbb{G}_1(s, S_h^j(s))ds, \\
E_h(t_{n+1}) &= E_{h_0} + \frac{\beta(1-\alpha)t_n^{\beta-1}\mathbb{G}_2(t_n, E_h(t_n))}{\mathbb{AB}(\alpha)} \\
&\quad + \frac{\alpha\beta}{\mathbb{AB}(\alpha)\Gamma(\alpha)}\sum_{j=1}^{n}\int_{t_j}^{t_{j+1}}(t_{j+1}-s)^{\alpha-1}s^{\beta-1}\mathbb{G}_2(s, E_h^j(s))ds, \\
I_h(t_{n+1}) &= I_{h_0} + \frac{\beta(1-\alpha)t_n^{\beta-1}\mathbb{G}_3(t_n, I_h(t_n))}{\mathbb{AB}(\alpha)} \\
&\quad + \frac{\alpha\beta}{\mathbb{AB}(\alpha)\Gamma(\alpha)}\sum_{j=1}^{n}\int_{t_j}^{t_{j+1}}(t_{j+1}-s)^{\alpha-1}s^{\beta-1}\mathbb{G}_3(s, I_h^j(s))ds, \\
Q_h(t_{n+1}) &= Q_{h_0} + \frac{\beta(1-\alpha)t_n^{\beta-1}\mathbb{G}_4(t_n, Q_h(t_n))}{\mathbb{AB}(\alpha)} \\
&\quad + \frac{\alpha\beta}{\mathbb{AB}(\alpha)\Gamma(\alpha)}\sum_{j=1}^{n}\int_{t_j}^{t_{j+1}}(t_{j+1}-s)^{\alpha-1}s^{\beta-1}\mathbb{G}_4(s, Q_h^j(s))ds, \\
R_h(t_{n+1}) &= R_{h_0} + \frac{\beta(1-\alpha)t_n^{\beta-1}\mathbb{G}_5(t_n, R_h(t_n))}{\mathbb{AB}(\alpha)} \\
&\quad + \frac{\alpha\beta}{\mathbb{AB}(\alpha)\Gamma(\alpha)}\sum_{j=1}^{n}\int_{t_j}^{t_{j+1}}(t_{j+1}-s)^{\alpha-1}s^{\beta-1}\mathbb{G}_5(s, R_h^j(s))ds, \\
S_r(t_{n+1}) &= S_{r_0} + \frac{\beta(1-\alpha)t_n^{\beta-1}\mathbb{G}_6(t_n, S_r(t_n))}{\mathbb{AB}(\alpha)} \\
&\quad + \frac{\alpha\beta}{\mathbb{AB}(\alpha)\Gamma(\alpha)}\sum_{j=1}^{n}\int_{t_j}^{t_{j+1}}(t_{j+1}-s)^{\alpha-1}s^{\beta-1}\mathbb{G}_6(s, S_r^j(s))ds, \\
E_r(t_{n+1}) &= E_{r_0} + \frac{\beta(1-\alpha)t_n^{\beta-1}\mathbb{G}_7(t_n, E_r(t_n))}{\mathbb{AB}(\alpha)} \\
&\quad + \frac{\alpha\beta}{\mathbb{AB}(\alpha)\Gamma(\alpha)}\sum_{j=1}^{n}\int_{t_j}^{t_{j+1}}(t_{j+1}-s)^{\alpha-1}s^{\beta-1}\mathbb{G}_7(s, E_r^j(s))ds,
\end{aligned}$$

$$I_r(t_{n+1}) = I_{r_0} + \frac{\beta(1-\alpha)t_n^{\beta-1}\mathbb{G}_8(t_n, I_r(t_n))}{\mathbb{AB}(\alpha)} + \frac{\alpha\beta}{\mathbb{AB}(\alpha)\Gamma(\alpha)}\sum_{j=1}^{n}\int_{t_j}^{t_{j+1}}(t_{j+1}-s)^{\alpha-1}s^{\beta-1}\mathbb{G}_8(s, I_r^j(s))ds.$$

Next, we use two-step Lagrange interpolation polynomials with $\Delta t = t_{j+1} - t_j$ to estimate the integrand functions on $[t_j, t_{j+1}]$. Thus, we have

$$\begin{aligned}
S_h(t_{n+1}) &= S_{h_0} + \frac{\beta(1-\alpha)t_n^{\beta-1}\mathbb{G}_1(t_n, S_h(t_n))}{\mathbb{AB}(\alpha)} + \frac{\alpha\beta}{\mathbb{AB}(\alpha)\Gamma(\alpha)}\sum_{j=1}^{n}\int_{t_j}^{t_{j+1}}(t_{j+1}-s)^{\alpha-1}s^{\beta-1}\mathcal{W}_j^{S_h}(s)ds,\\
E_h(t_{n+1}) &= E_{h_0} + \frac{\beta(1-\alpha)t_n^{\beta-1}\mathbb{G}_2(t_n, E_h(t_n))}{\mathbb{AB}(\alpha)} + \frac{\alpha\beta}{\mathbb{AB}(\alpha)\Gamma(\alpha)}\sum_{j=1}^{n}\int_{t_j}^{t_{j+1}}(t_{j+1}-s)^{\alpha-1}s^{\beta-1}\mathcal{W}_j^{E_h}(s)ds,\\
I_h(t_{n+1}) &= I_{h_0} + \frac{\beta(1-\alpha)t_n^{\beta-1}\mathbb{G}_3(t_n, I_h(t_n))}{\mathbb{AB}(\alpha)} + \frac{\alpha\beta}{\mathbb{AB}(\alpha)\Gamma(\alpha)}\sum_{j=1}^{n}\int_{t_j}^{t_{j+1}}(t_{j+1}-s)^{\alpha-1}s^{\beta-1}\mathcal{W}_j^{I_h}(s)ds,\\
Q_h(t_{n+1}) &= Q_{h_0} + \frac{\beta(1-\alpha)t_n^{\beta-1}\mathbb{G}_4(t_n, Q_h(t_n))}{\mathbb{AB}(\alpha)} + \frac{\alpha\beta}{\mathbb{AB}(\alpha)\Gamma(\alpha)}\sum_{j=1}^{n}\int_{t_j}^{t_{j+1}}(t_{j+1}-s)^{\alpha-1}s^{\beta-1}\mathcal{W}_j^{Q_h}(s)ds,\\
R_h(t_{n+1}) &= R_{h_0} + \frac{\beta(1-\alpha)t_n^{\beta-1}\mathbb{G}_5(t_n, R_h(t_n))}{\mathbb{AB}(\alpha)} + \frac{\alpha\beta}{\mathbb{AB}(\alpha)\Gamma(\alpha)}\sum_{j=1}^{n}\int_{t_j}^{t_{j+1}}(t_{j+1}-s)^{\alpha-1}s^{\beta-1}\mathcal{W}_j^{R_h}(s)ds,\\
S_r(t_{n+1}) &= S_{r_0} + \frac{\beta(1-\alpha)t_n^{\beta-1}\mathbb{G}_6(t_n, S_r(t_n))}{\mathbb{AB}(\alpha)} + \frac{\alpha\beta}{\mathbb{AB}(\alpha)\Gamma(\alpha)}\sum_{j=1}^{n}\int_{t_j}^{t_{j+1}}(t_{j+1}-s)^{\alpha-1}s^{\beta-1}\mathcal{W}_j^{S_r}(s)ds,\\
E_r(t_{n+1}) &= E_{r_0} + \frac{\beta(1-\alpha)t_n^{\beta-1}\mathbb{G}_7(t_n, E_r(t_n))}{\mathbb{AB}(\alpha)} + \frac{\alpha\beta}{\mathbb{AB}(\alpha)\Gamma(\alpha)}\sum_{j=1}^{n}\int_{t_j}^{t_{j+1}}(t_{j+1}-s)^{\alpha-1}s^{\beta-1}\mathcal{W}_j^{E_r}(s)ds,\\
I_r(t_{n+1}) &= I_{r_0} + \frac{\beta(1-\alpha)t_n^{\beta-1}\mathbb{G}_8(t_n, I_r(t_n))}{\mathbb{AB}(\alpha)} + \frac{\alpha\beta}{\mathbb{AB}(\alpha)\Gamma(\alpha)}\sum_{j=1}^{n}\int_{t_j}^{t_{j+1}}(t_{j+1}-s)^{\alpha-1}s^{\beta-1}\mathcal{W}_j^{I_r}(s)ds,
\end{aligned}$$

where

$$\begin{aligned}
\mathcal{W}_j^{S_h}(s) &= \frac{s-t_{j-1}}{t_j-t_{j-1}}t_j^{\beta-1}\mathbb{G}_1(s, S_h^j(s)) - \frac{s-t_{j-1}}{t_j-t_{j-1}}t_{j-1}^{\beta-1}\mathbb{G}_1(s, S_h^{j-1}(s)),\\
\mathcal{W}_j^{E_h}(s) &= \frac{s-t_{j-1}}{t_j-t_{j-1}}t_j^{\beta-1}\mathbb{G}_2(s, E_h^j(s)) - \frac{s-t_{j-1}}{t_j-t_{j-1}}t_{j-1}^{\beta-1}\mathbb{G}_2(s, E_h^{j-1}(s)),\\
\mathcal{W}_j^{I_h}(s) &= \frac{s-t_{j-1}}{t_j-t_{j-1}}t_j^{\beta-1}\mathbb{G}_3(s, I_h^j(s)) - \frac{s-t_{j-1}}{t_j-t_{j-1}}t_{j-1}^{\beta-1}\mathbb{G}_3(s, I_h^{j-1}(s)),\\
\mathcal{W}_j^{R_h}(s) &= \frac{s-t_{j-1}}{t_j-t_{j-1}}t_j^{\beta-1}\mathbb{G}_4(s, R_h^j(s)) - \frac{s-t_{j-1}}{t_j-t_{j-1}}t_{j-1}^{\beta-1}\mathbb{G}_4(s, R_h^{j-1}(s)),\\
\mathcal{W}_j^{Q_h}(s) &= \frac{s-t_{j-1}}{t_j-t_{j-1}}t_j^{\beta-1}\mathbb{G}_5(s, Q_h^j(s)) - \frac{s-t_{j-1}}{t_j-t_{j-1}}t_{j-1}^{\beta-1}\mathbb{G}_5(s, Q_h^{j-1}(s)),
\end{aligned}$$

$$
\begin{aligned}
\mathcal{W}_j^{S_r}(s) &= \frac{s-t_{j-1}}{t_j-t_{j-1}}t_j^{\beta-1}\mathbb{G}_6(s,S_r^j(s)) - \frac{s-t_{j-1}}{t_j-t_{j-1}}t_{j-1}^{\beta-1}\mathbb{G}_6(s,S_r^{j-1}(s)),\\
\mathcal{W}_j^{E_r}(s) &= \frac{s-t_{j-1}}{t_j-t_{j-1}}t_j^{\beta-1}\mathbb{G}_7(s,E_r^j(s)) - \frac{s-t_{j-1}}{t_j-t_{j-1}}t_{j-1}^{\beta-1}\mathbb{G}_7(s,E_r^{j-1}(s)),\\
\mathcal{W}_j^{I_r}(s) &= \frac{s-t_{j-1}}{t_j-t_{j-1}}t_j^{\beta-1}\mathbb{G}_8(s,I_r^j(s)) - \frac{s-t_{j-1}}{t_j-t_{j-1}}t_{j-1}^{\beta-1}\mathbb{G}_8(s,I_r^{j-1}(s)).
\end{aligned}
$$

Finally, we achieve schemes that yield the numerical results to the $\mathbb{FF}$-$\mathbb{MPX}$ model (2.8)

$$
\begin{aligned}
S_h(t_{n+1}) &= S_{h_0} + \frac{\beta(1-\alpha)t_n^{\beta-1}\mathbb{G}_1(t_n,S_h(t_n))}{\mathbb{AB}(\alpha)}\\
&\quad + \frac{\beta(\Delta t)^\alpha}{\mathbb{AB}(\alpha)\Gamma(\alpha+2)}\sum_{j=1}^{n}\Big[t_j^{\beta-1}\mathbb{G}_1(s,S_h^j(s))\Upsilon_1(n,j) - t_{j-1}^{\beta-1}\mathbb{G}_1(t_j,S_h^{j-1}(s))\Upsilon_2(n,j)\Big],\\
E_h(t_{n+1}) &= E_{h_0} + \frac{\beta(1-\alpha)t_n^{\beta-1}\mathbb{G}_2(t_n,E_h(t_n))}{\mathbb{AB}(\alpha)}\\
&\quad + \frac{\beta(\Delta t)^\alpha}{\mathbb{AB}(\alpha)\Gamma(\alpha+2)}\sum_{j=1}^{n}\Big[t_j^{\beta-1}\mathbb{G}_2(s,E_h^j(s))\Upsilon_1(n,j) - t_{j-1}^{\beta-1}\mathbb{G}_2(t_j,E_h^{j-1}(s))\Upsilon_2(n,j)\Big],\\
I_h(t_{n+1}) &= I_{h_0} + \frac{\beta(1-\alpha)t_n^{\beta-1}\mathbb{G}_3(t_n,I_h(t_n))}{\mathbb{AB}(\alpha)}\\
&\quad + \frac{\beta(\Delta t)^\alpha}{\mathbb{AB}(\alpha)\Gamma(\alpha+2)}\sum_{j=1}^{n}\Big[t_j^{\beta-1}\mathbb{G}_3(s,I_h^j(s))\Upsilon_1(n,j) - t_{j-1}^{\beta-1}\mathbb{G}_3(t_j,I_hj-1(s))\Upsilon_2(n,j)\Big],\\
Q_h(t_{n+1}) &= Q_{h_0} + \frac{\beta(1-\alpha)t_n^{\beta-1}\mathbb{G}_4(t_n,Q_h(t_n))}{\mathbb{AB}(\alpha)}\\
&\quad + \frac{\beta(\Delta t)^\alpha}{\mathbb{AB}(\alpha)\Gamma(\alpha+2)}\sum_{j=1}^{n}\Big[t_j^{\beta-1}\mathbb{G}_4(s,Q_h^j(s))\Upsilon_1(n,j) - t_{j-1}^{\beta-1}\mathbb{G}_4(t_j,Q_h^{j-1}(s))\Upsilon_2(n,j)\Big],\\
R_h(t_{n+1}) &= R_{h_0} + \frac{\beta(1-\alpha)t_n^{\beta-1}\mathbb{G}_5(t_n,R_h(t_n))}{\mathbb{AB}(\alpha)}\\
&\quad + \frac{\beta(\Delta t)^\alpha}{\mathbb{AB}(\alpha)\Gamma(\alpha+2)}\sum_{j=1}^{n}\Big[t_j^{\beta-1}\mathbb{G}_5(s,R_h^j(s))\Upsilon_1(n,j) - t_{j-1}^{\beta-1}\mathbb{G}_5(t_j,R_h^{j-1}(s))\Upsilon_2(n,j)\Big],\\
S_r(t_{n+1}) &= S_{r_0} + \frac{\beta(1-\alpha)t_n^{\beta-1}\mathbb{G}_6(t_n,S_r(t_n))}{\mathbb{AB}(\alpha)}\\
&\quad + \frac{\beta(\Delta t)^\alpha}{\mathbb{AB}(\alpha)\Gamma(\alpha+2)}\sum_{j=1}^{n}\Big[t_j^{\beta-1}\mathbb{G}_6(s,S_r^j(s))\Upsilon_1(n,j) - t_{j-1}^{\beta-1}\mathbb{G}_6(t_j,S_r^{j-1}(s))\Upsilon_2(n,j)\Big],\\
E_r(t_{n+1}) &= E_{r_0} + \frac{\beta(1-\alpha)t_n^{\beta-1}\mathbb{G}_7(t_n,E_r(t_n))}{\mathbb{AB}(\alpha)}\\
&\quad + \frac{\beta(\Delta t)^\alpha}{\mathbb{AB}(\alpha)\Gamma(\alpha+2)}\sum_{j=1}^{n}\Big[t_j^{\beta-1}\mathbb{G}_7(s,E_r^j(s))\Upsilon_1(n,j) - t_{j-1}^{\beta-1}\mathbb{G}_7(t_j,E_r^{j-1}(s))\Upsilon_2(n,j)\Big],
\end{aligned}
$$

$$I_r(t_{n+1}) = I_{r_0} + \frac{\beta(1-\alpha)t_n^{\beta-1}\mathbb{G}_8(t_n, I_r(t_n))}{\mathbb{AB}(\alpha)} + \frac{\beta(\Delta t)^\alpha}{\mathbb{AB}(\alpha)\Gamma(\alpha+2)}\sum_{j=1}^{n}\left[t_j^{\beta-1}\mathbb{G}_8(s, I_r^j(s))\Upsilon_1(n,j) - t_{j-1}^{\beta-1}\mathbb{G}_8(t_j, I_r^{j-1}(s))\Upsilon_2(n,j)\right],$$

where $\Upsilon_1(n,j) = (n+1-j)^\alpha(n-j+2+\alpha) - (n-j)^\alpha(n-j+2+2\alpha)$ and $\Upsilon_2(n,j) = (n+1-j)^{\alpha+1} - (n-j)^\alpha(n-j+1+\alpha)$.

6. Results and discussions

This section shows some simulation results of the $\mathbb{FF}$-$\mathbb{MPX}$ model (2.8) at different parameters to illustrate our results. Various models have been extended to simulate infectious diseases caused by the $\mathbb{MPX}$ virus. A fractional differential system is utilized to describe the dynamic behavior in these models. To provide greater precision and accuracy than previous results, this work represents the considered model with a system of fractional differential equations. The fractional differential equations allow us to change the order of the fractional derivative to better match the real data. This paper will be shown graphically simulations separated by considering two equilibrium points, namely $\mathfrak{E}_0^*$ and $\mathfrak{E}_1^*$, separately to observe the impacts of variables on the dynamics of the $\mathbb{FF}$-$\mathbb{MPX}$ model. We achieve the results shown in Figures 2–17 by performing the stated procedure with the indicated parameters' values as in Table 2. Figures 2–9 show the results for the point $\mathfrak{E}_0^*$, while the results for the point $\mathfrak{E}_1^*$ are shown in Figures 10–17.

Table 2. Parameter values utilized of the $\mathbb{MPX}$ model (2.7) for $\mathfrak{E}_0^*$ and $\mathfrak{E}_1^*$.

$\mathfrak{E}_0^*$			$\mathfrak{E}_1^*$		
Parameter	Value, $Year^{-1}$	Source	Parameter	Value, $Year^{-1}$	Source
Λ_h	0.029	[46]	Λ_h	0.029	[46]
Λ_r	0.2	[46]	Λ_r	0.9	[48]
b_1	0.00025	[13]	b_1	0.000009	[48]
b_2	0.00006	[13]	b_2	0.99	Assumed
b_3	0.027	[13]	b_3	0.0057	[48]
a_1	0.2	Assumed	a_1	0.007	[48]
a_2	2.0	Estimated	a_2	0.0081	[48]
a_3	0.007	Estimated	a_3	0.007	[48]
θ	2.0	Estimated	θ	0.029	[48]
τ	0.52	Assumed	τ	0.012	[48]
ν	0.83	[46]	ν	0.056	[48]
μ_h	1.5	[13]	μ_h	0.05	[49]
μ_r	0.002	[13]	μ_r	0.002	[40]
δ_h	0.2	[47]	δ_h	0.00008	[48]
δ_r	0.5	Assumed	δ_r	0.0001	[48]

Case 1. We apply all parameter values presented in Table 2 for $\mathfrak{E}_0^*$. This case obtains the values $\mathfrak{R}_0 = 1.2819 \times 10^{-6} < 1$ and the condition $K_4K_5 - a_3b_3 = 0.0043 > 0$, which satisfy all assumptions of Theorem 3.2. Therefore, the equilibrium $\mathfrak{E}_0^* = (0.0193, 0, 0, 0, 0, 100, 0, 0)$ is locally asymptotically stable. In addition, we apply the numerical schemes from Section 5 to show the numerical simulations. This yields the approximate solutions of the $\mathbb{FF}$-$\mathbb{MPX}$ model (2.8) for various values of α and β with the initial condition is $(800, 5, 5, 5, 0, 500, 125, 20)$ as in the distinguished consideration. Figures 2 and 3 show the behaviors of each group in the $\mathbb{FF}$-$\mathbb{MPX}$ model (2.8) when $\alpha = 1$ is fixed and β is varied where $\beta \in \{1.00, 0.96, 0.92, 0.88, 0.84\}$. Figures 4 and 5 describe the behaviors of all groups for the proposed model when α is varied where $\alpha \in \{1.00, 0.96, 0.92, 0.88, 0.84\}$ and $\beta = 1$ is fixed. The behaviors of each group when α and β are varied equally that is $\alpha \in \{0.84, 0.88, 0.92, 0.96, 1.00\}$ and $\beta \in \{0.84, 0.88, 0.92, 0.96, 1.00\}$ are shown in Figures 6 and 7. At last of subcase, when α and β are varied differently, that is, $\alpha \in \{0.84, 0.88, 0.92, 0.96, 1.00\}$ and $\beta \in \{1.00, 0.96, 0.92, 0.88, 0.84\}$ are presented in Figures 8 and 9. From each variety of subcases, it can be seen from Figures 2–9 that all the graphs of each group show the same trend. The behaviors of human groups such as susceptible, exposed, infected, isolated, and the behaviors of rodent groups such as susceptible, exposed, and infected gradually decrease from the start day and then steadily reach the steady state $\mathfrak{E}_0^*$. Furthermore, the behavior of the recovered humans quickly increases from the start day and then suddenly decreases until it approaches zero in the disease-free situation. Moreover, in the last subcase, when α and β vary reversely, the graph shows that the stability-reaching time is used over a longer length if compared with the previous cases.

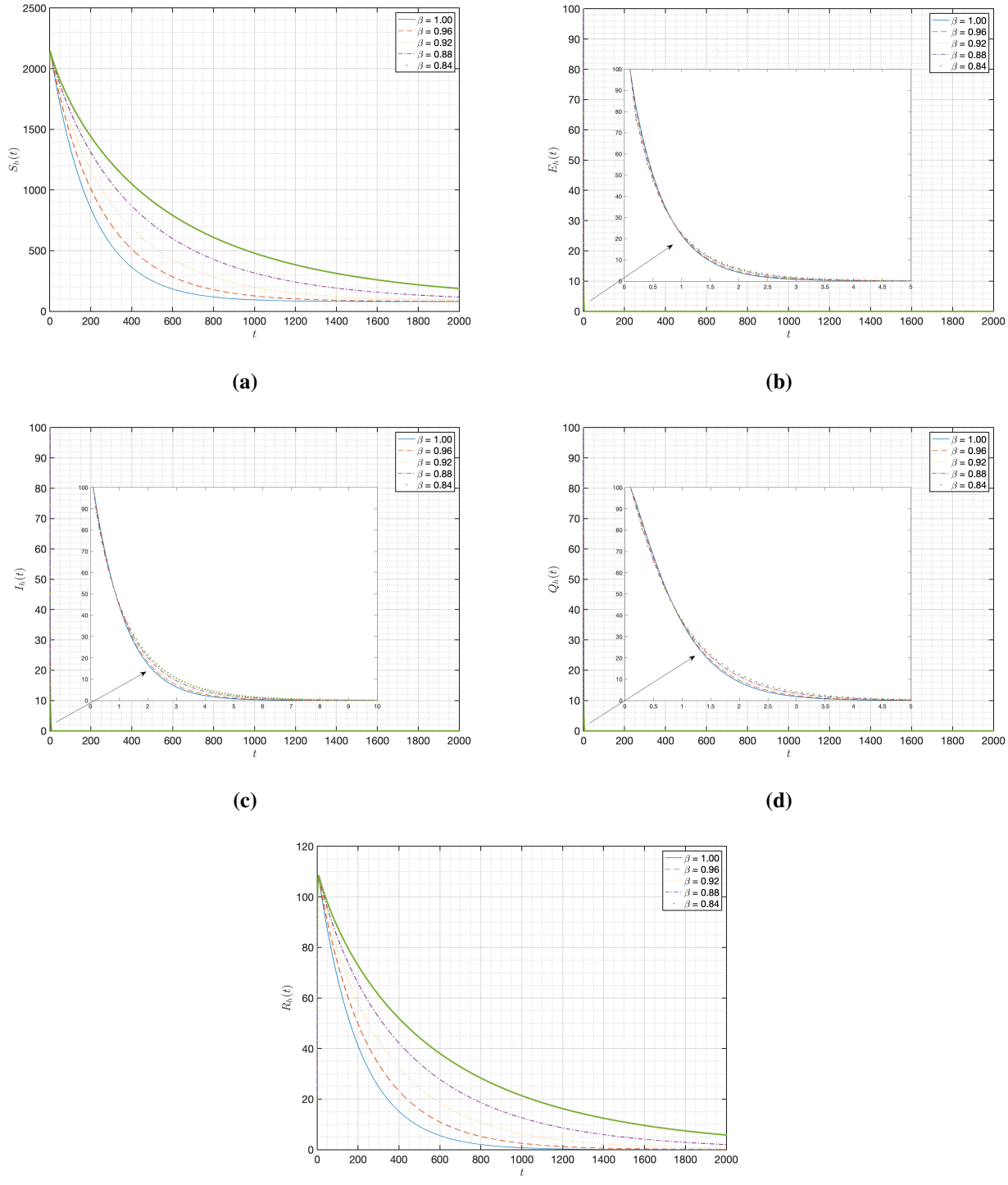

Figure 2. Numerical results of $S_h(t)$, $E_h(t)$, $I_h(t)$, $Q_h(t)$, and $R_h(t)$ of the $\mathbb{FF}$-$\mathbb{MPX}$ model (2.8) when $\alpha = 1.00$ and $\beta \in \{0.84, 0.88, 0.92, 0.96, 1.00\}$ in case of $\mathfrak{E}_0^*$.

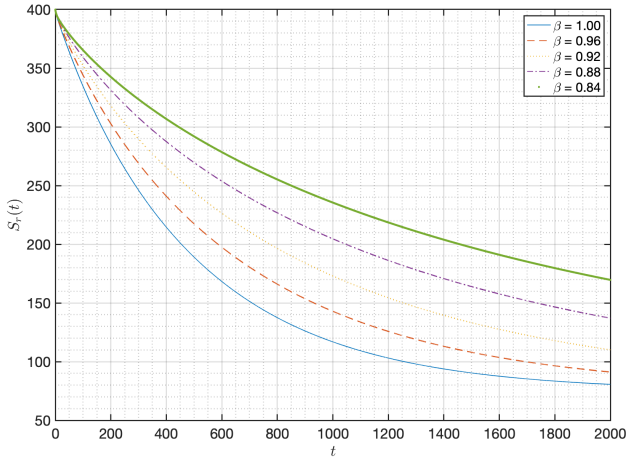

(a)

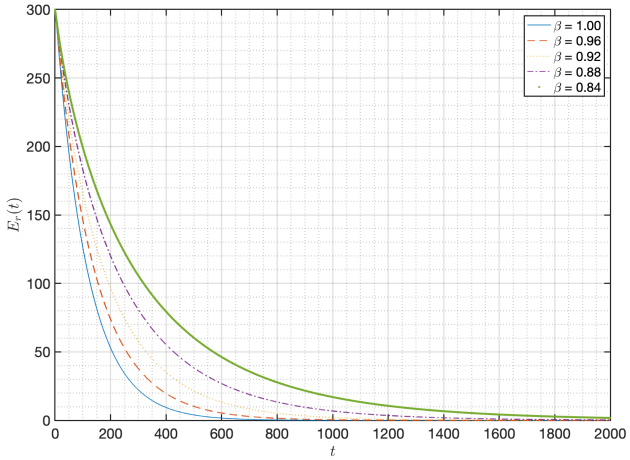

(b)

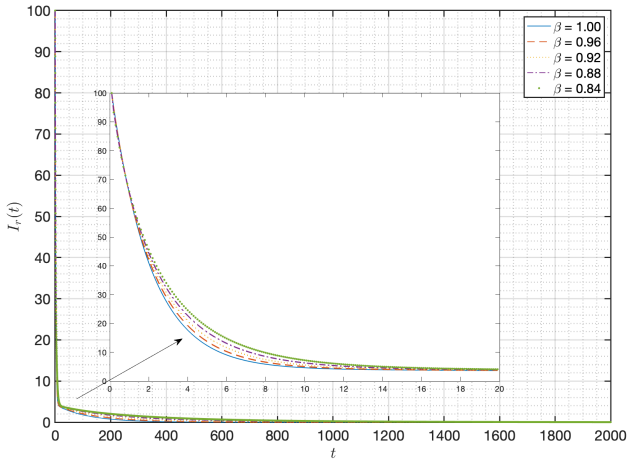

(c)

Figure 3. Numerical results of $S_r(t)$, $E_r(t)$, and $I_r(t)$ of the $\mathbb{FF}$-$\mathbb{MPX}$ model (2.8) when $\alpha = 1.00$ and $\beta \in \{0.84, 0.88, 0.92, 0.96, 1.00\}$ in case of $\mathfrak{E}_0^*$.

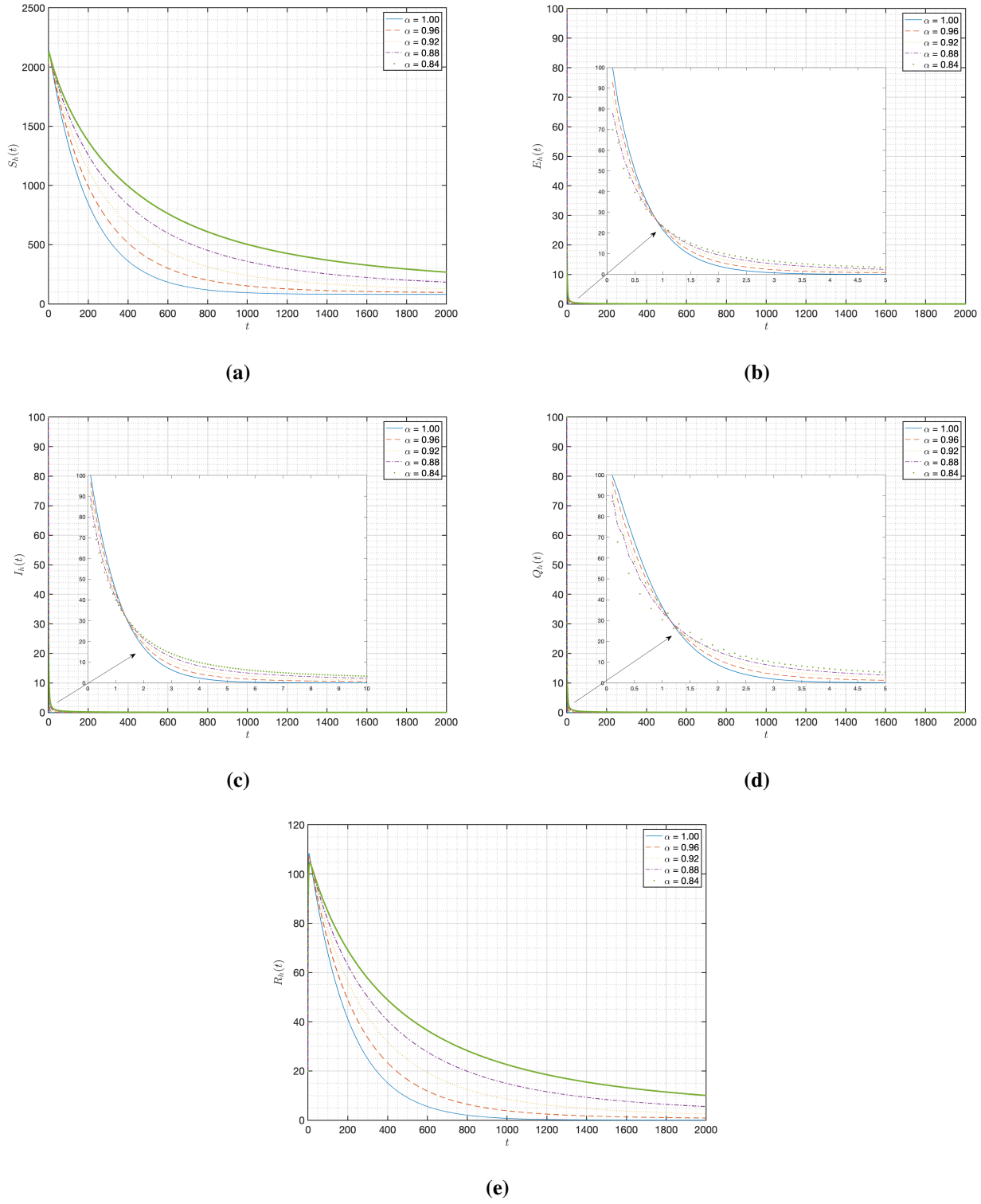

Figure 4. Numerical results of $S_h(t)$, $E_h(t)$, $I_h(t)$, $Q_h(t)$, and $R_h(t)$ of the $\mathbb{FF}$-$\mathbb{MPX}$ model (2.8) when $\alpha \in \{0.84, 0.88, 0.92, 0.96, 1.00\}$ and $\beta = 1.00$ in case of $\mathfrak{E}_0^*$.

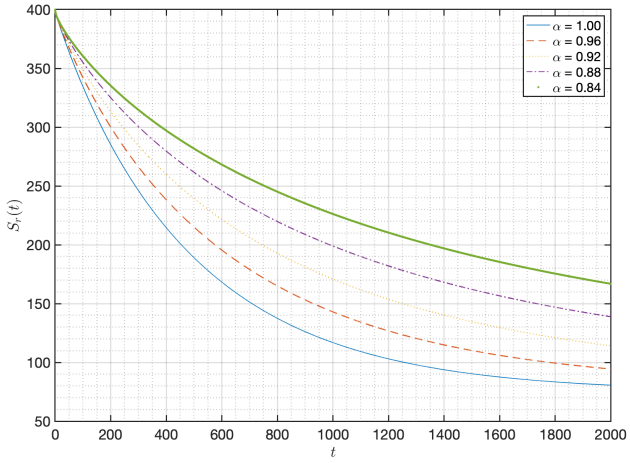

(a)

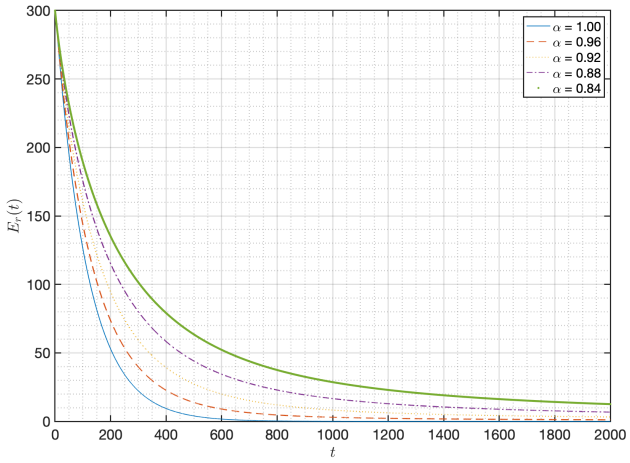

(b)

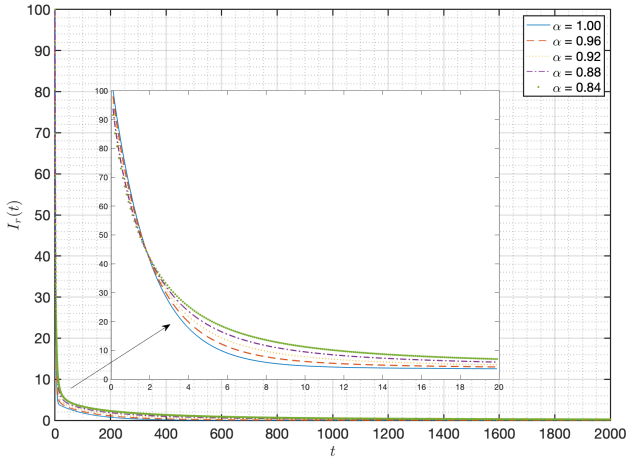

(c)

Figure 5. Numerical results of $S_r(t)$, $E_r(t)$, and $I_r(t)$ of the $\mathbb{FF}$-$\mathbb{MPX}$ model (2.8) when $\alpha \in \{0.84, 0.88, 0.92, 0.96, 1.00\}$ and $\beta = 1.00$ in case of $\mathfrak{E}_0^*$.

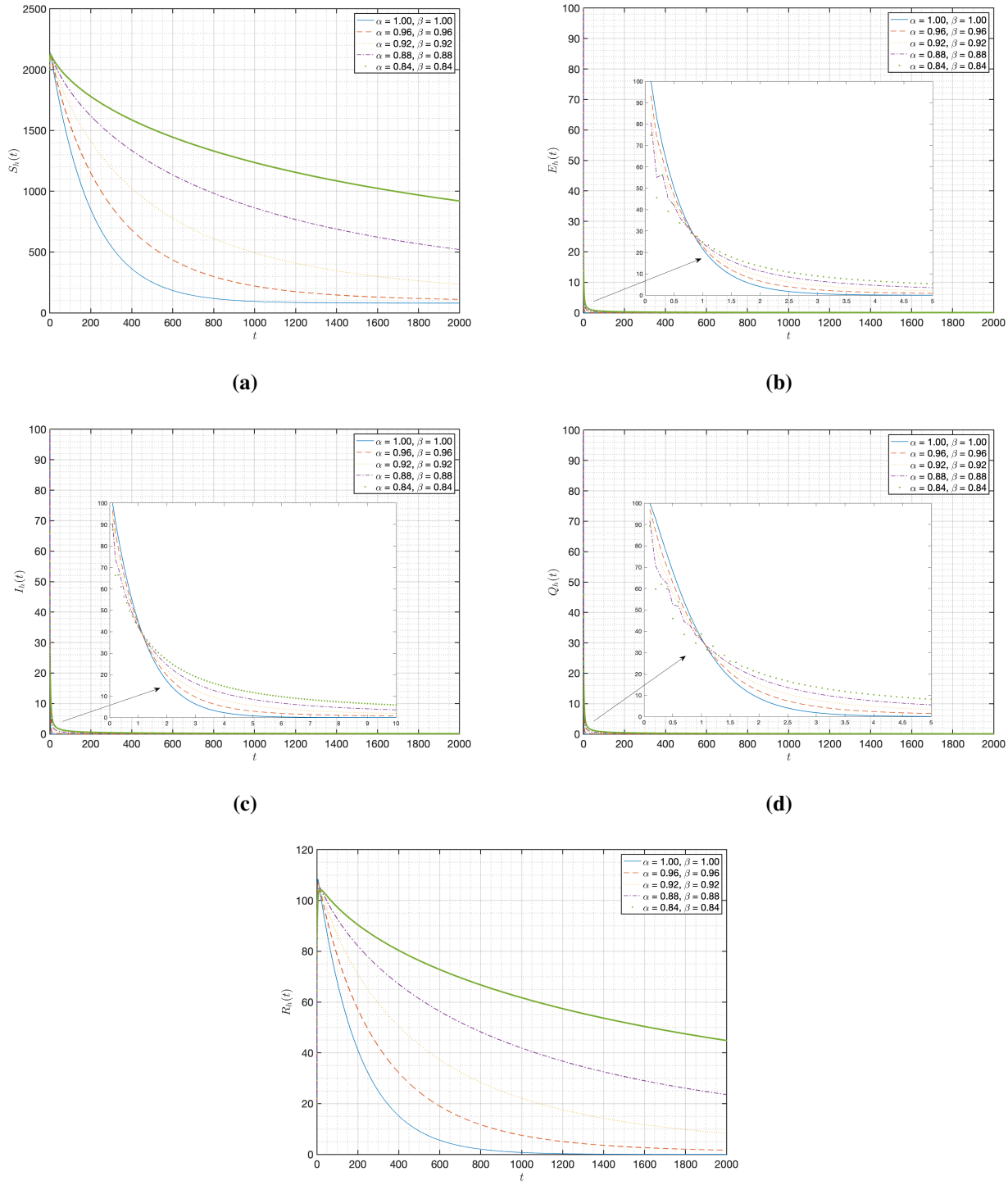

Figure 6. Numerical results of $S_h(t)$, $E_h(t)$, $I_h(t)$, $Q_h(t)$, and $R_h(t)$ of the $\mathbb{FF}$-$\mathbb{MPX}$ model (2.8) when $\alpha \in \{0.84, 0.88, 0.92, 0.96, 1.00\}$ and $\beta \in \{0.84, 0.88, 0.92, 0.96, 1.00\}$ in case of $\mathfrak{E}_0^*$.

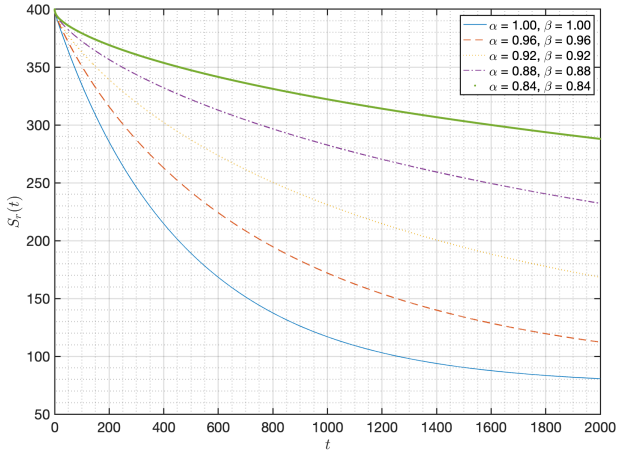

(a)

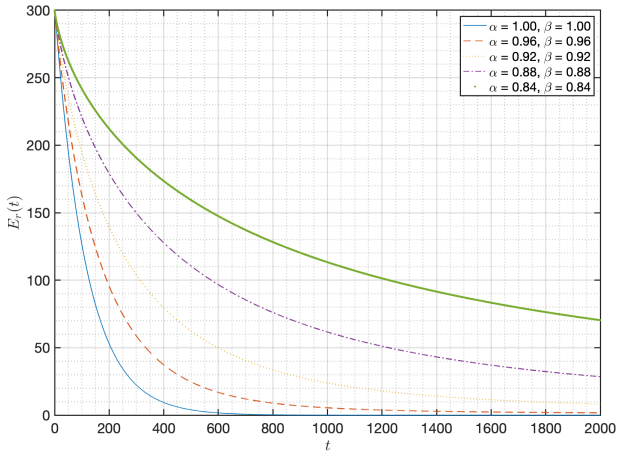

(b)

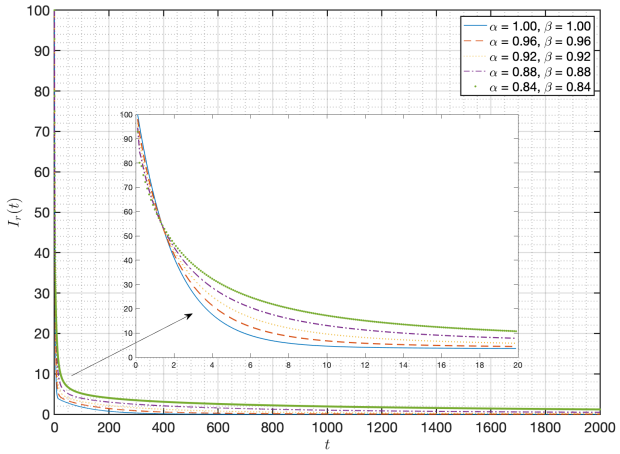

(c)

Figure 7. Numerical results of $S_r(t)$, $E_r(t)$, and $I_r(t)$ of the $\mathbb{FF}$-$\mathbb{MPX}$ model (2.8) when $\alpha \in \{0.84, 0.88, 0.92, 0.96, 1.00\}$ and $\beta \in \{0.84, 0.88, 0.92, 0.96, 1.00\}$ in case of $\mathfrak{E}_0^*$.

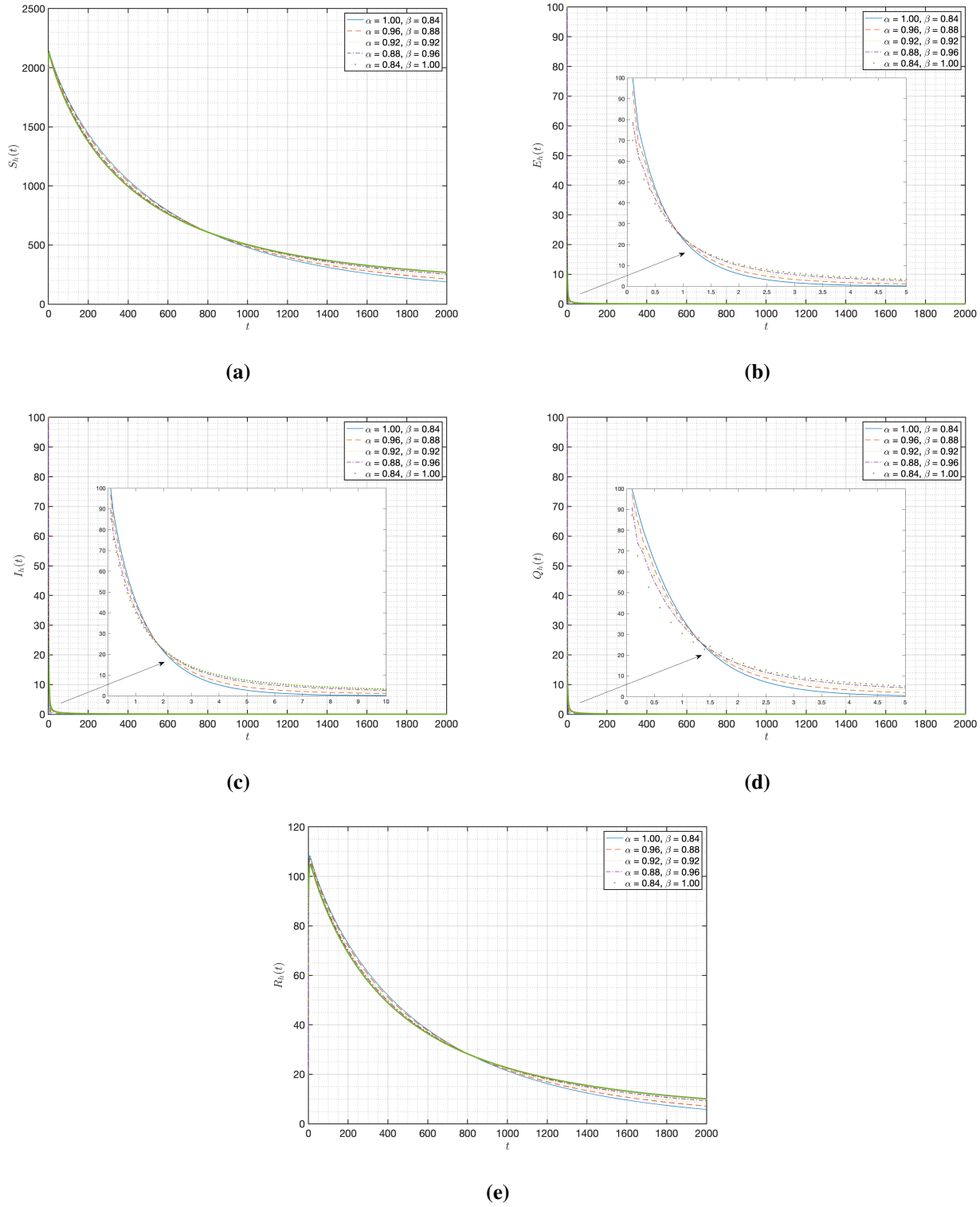

Figure 8. Numerical results of $S_h(t)$, $E_h(t)$, $I_h(t)$, $Q_h(t)$, and $R_h(t)$ of the $\mathbb{FF}$-$\mathbb{MPX}$ model (2.8) when $\alpha \in \{0.84, 0.88, 0.92, 0.96, 1.00\}$ and $\beta \in \{1.00, 0.96, 0.92, 0.88, 0.84\}$ in case of $\mathfrak{E}_0^*$.

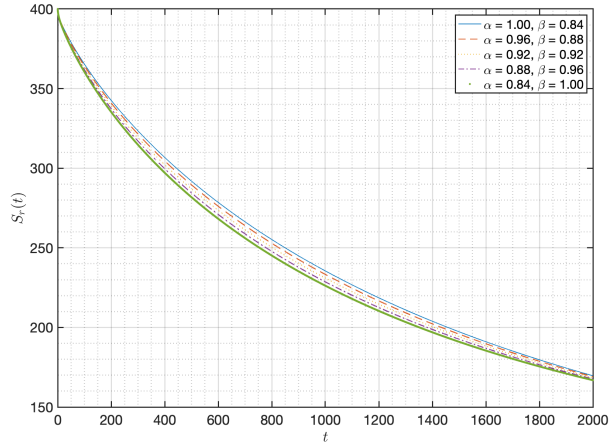

(a)

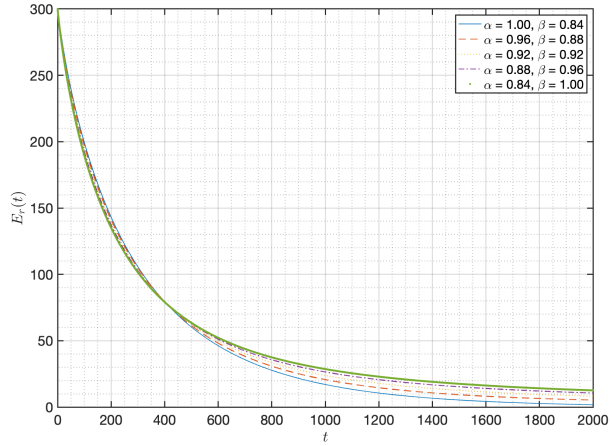

(b)

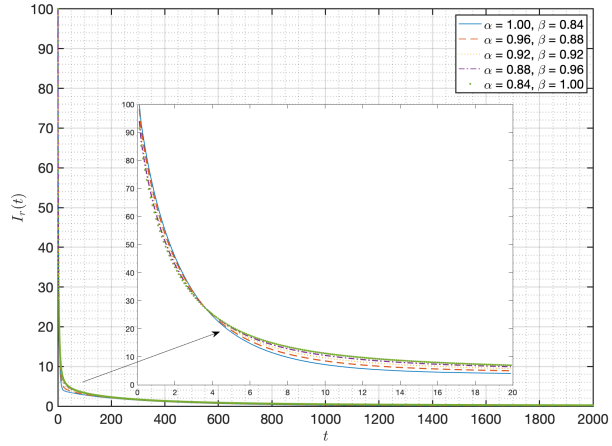

(c)

Figure 9. Numerical results of $S_h(t)$, $E_h(t)$, $I_h(t)$, $Q_h(t)$, $R_h(t)$, $S_r(t)$, $E_r(t)$, and $I_r(t)$ of the $\mathbb{FF}$-$\mathbb{MPX}$ model (2.8) when $\alpha \in \{0.84, 0.88, 0.92, 0.96, 1.00\}$ and $\beta \in \{1.00, 0.96, 0.92, 0.88, 0.84\}$ in case of $\mathfrak{E}_0^*$.

Case 2. We apply all parameter values presented in Table 2 for $\mathfrak{E}_1^*$. This case obtains the values $\Re_0 = 1.0035 > 1$, $\mathcal{A}_1 = 3.4125 \times 10^{-1}$, $\mathcal{A}_2 = 3.874 \times 10^{-2}$, $\mathcal{A}_3 = 1.82 \times 10^{-3}$, $\mathcal{A}_4 = 3.5977 \times 10^{-5}$, $\mathcal{A}_5 = 2.87971 \times 10^{-7}$, $\mathcal{A}_6 = 7.54937 \times 10^{-10}$, $\mathcal{A}_7 = 6.37675 \times 10^{-13}$, $\mathcal{B}_1 = 3.342 \times 10^{-2}$, $\mathcal{B}_2 = 3.51331 \times 10^{-5}$, $\mathcal{B}_3 = 7.53069 \times 10^{-10}$, $\mathcal{C}_1 = 1.46 \times 10^{-3}$, $\mathcal{C}_2 = 2.80283 \times 10^{-7}$, $\mathcal{C}_3 = 6.37675 \times 10^{-13}$, $\mathcal{D}_1 = 2.8701 \times 10^{-5}$, $\mathcal{D}_2 = 7.38435 \times 10^{-10}$, $\mathcal{E}_1 = 2.4281 \times 10^{-7}$, $\mathcal{E}_2 = 6.37675 \times 10^{-13}$, and $\mathcal{F}_1 = 6.6306 \times 10^{-10}$. The conditions $\mathcal{A}_1 > 0$, $\mathcal{A}_7 > 0$, $\mathcal{A}_1\mathcal{A}_2 > \mathcal{A}_3$, $\mathcal{A}_1\mathcal{A}_2\mathcal{A}_3 + \mathcal{A}_1\mathcal{A}_5 > \mathcal{A}_1^2\mathcal{A}_4 + \mathcal{A}_3^2$, $\mathcal{B}_2\mathcal{C}_1 > \mathcal{B}_1\mathcal{C}_2$, $\mathcal{C}_2\mathcal{D}_1 > \mathcal{C}_1\mathcal{D}_2$, and $\mathcal{D}_2\mathcal{E}_1 > \mathcal{D}_1\mathcal{E}_2$ are satisfied all all assumptions of Theorem 3.3. Hence, the point $\mathfrak{E}_1^* = (0.46001, 0.09596, 0.00633, 0.00853, 0.00914, 208.92857, 53.57143, 178.57143)$ is locally asymptotically stable. Furthermore, we apply the numerical schemes in Section 5 to show the numerical simulations, which implies that the approximate solutions of the $\mathbb{FF}$-$\mathbb{MPX}$ model (2.8) for various values of α and β with the initial condition $(800, 5, 5, 5, 0, 500, 125, 20)$ as in the distinguished consideration. In this case, we consider the same subcase as Case 1. When $\alpha = 1$ and β is varied where $\beta \in \{1.00, 0.96, 0.92, 0.88, 0.84\}$, Figures 10 and 11 show the behaviors of each group in the $\mathbb{FF}$-$\mathbb{MPX}$ model (2.8). When α is varied where $\alpha \in \{1.00, 0.96, 0.92, 0.88, 0.84\}$ and $\beta = 1$ is fixed, the graph showing the behaviors of the considered model is shown in Figures 12 and 13. The varied equally of both α and β as $\alpha \in \{0.84, 0.88, 0.92, 0.96, 1.00\}$ and $\beta \in \{0.84, 0.88, 0.92, 0.96, 1.00\}$ are discussed as seen in Figures 14 and 15, while the varied differently that is $\alpha \in \{0.84, 0.88, 0.92, 0.96, 1.00\}$ and $\beta \in \{1.00, 0.96, 0.92, 0.88, 0.84\}$ are also considered as seen in Figures 16–17. Figures 10–17 show the behavior of the five groups of humans and three groups of rodents, and it is noticeable that they have pretty similar patterns for each subcase. All reach the equilibrium point $\mathfrak{E}_1^*$ when the time approaches infinity but spend different time points, where the last subcase spends the longest time compared to the others. Besides, it can be seen from the graphs that the behavior of the susceptible human, the infected human, the isolated human, the susceptible rodent, and the exposed rodent rapidly decreased from the beginning. Moreover, the behavior of the exposed humans, the recovered humans, and the infected rodents suddenly increased and decreased before reaching the referred steady state as time passed.

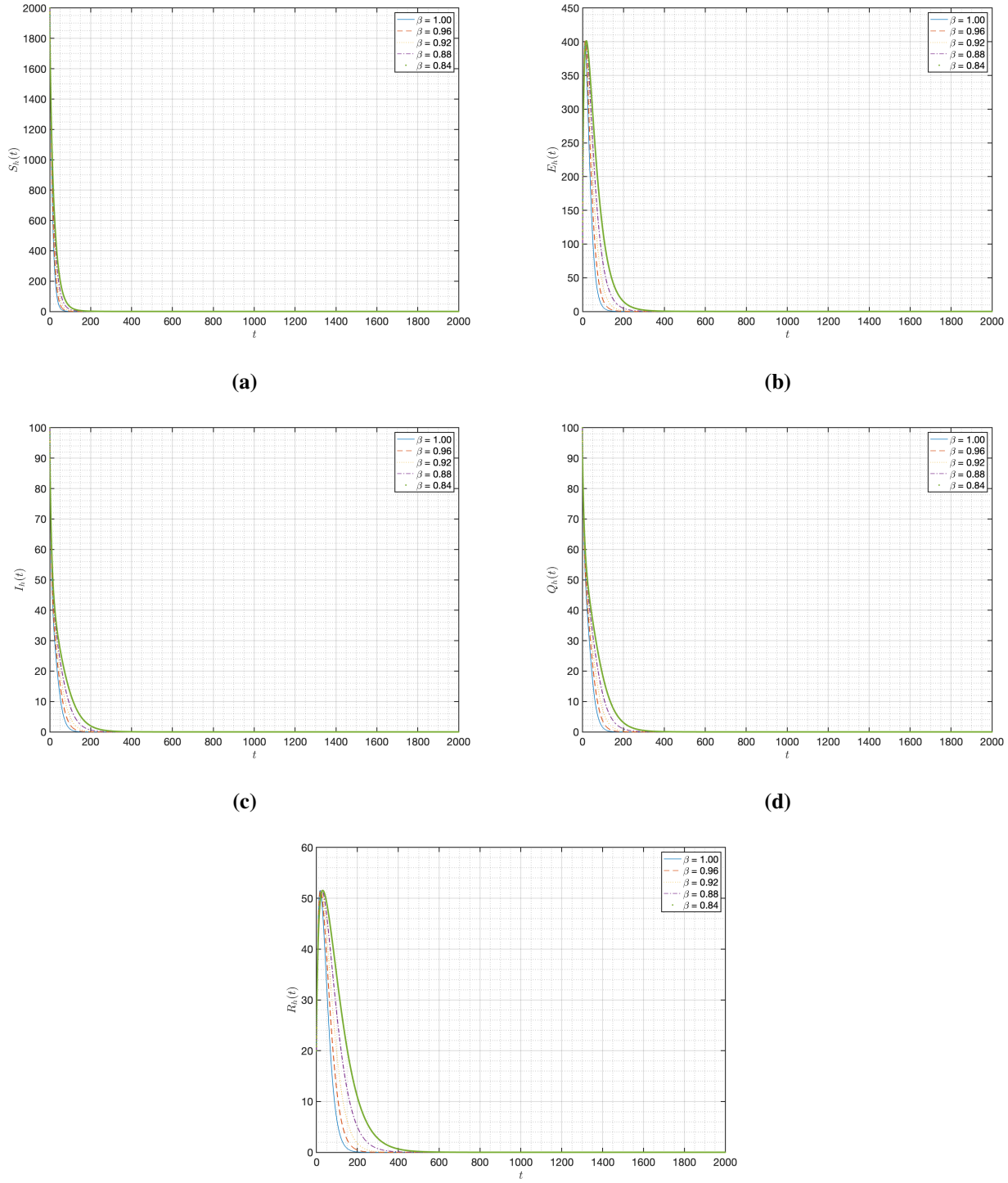

Figure 10. Numerical results of $S_h(t)$, $E_h(t)$, $I_h(t)$, $Q_h(t)$, and $R_h(t)$ of the $\mathbb{FF}$-$\mathbb{MPX}$ model (2.8) when $\alpha = 1.00$ and $\beta \in \{0.84, 0.88, 0.92, 0.96, 1.00\}$ in case of $\mathfrak{C}_1^*$.

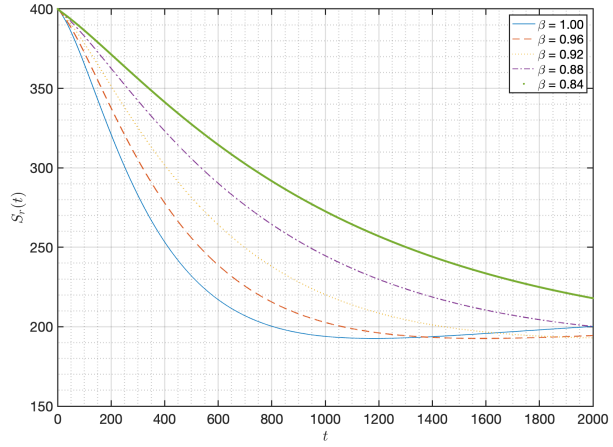

(a)

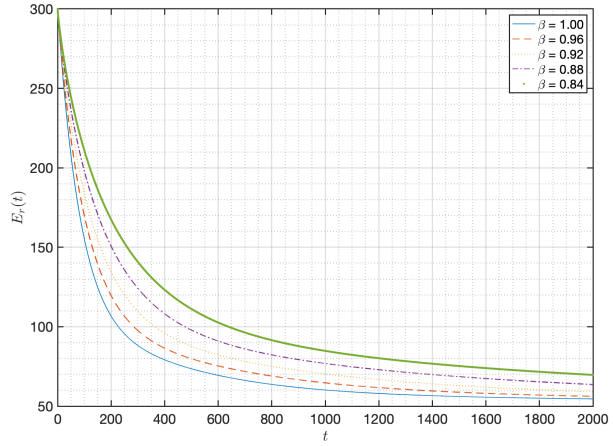

(b)

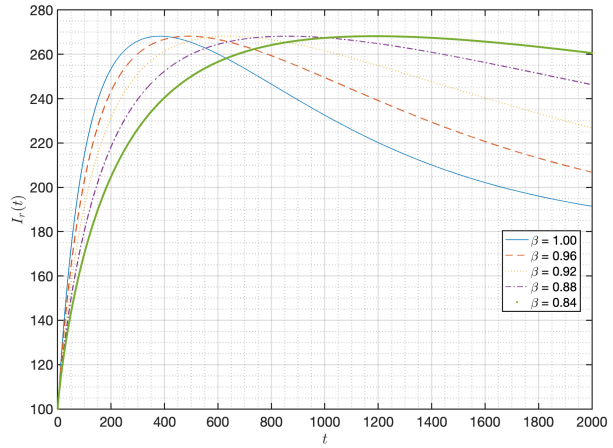

(c)

Figure 11. Numerical results of $S_h(t)$, $E_h(t)$, $I_h(t)$, $Q_h(t)$, $R_h(t)$, $S_r(t)$, $E_r(t)$, and $I_r(t)$ of the $\mathbb{FF}$-$\mathbb{MPX}$ model (2.8) when $\alpha = 1.00$ and $\beta \in \{0.84, 0.88, 0.92, 0.96, 1.00\}$ in case of $\mathfrak{E}_1^*$.

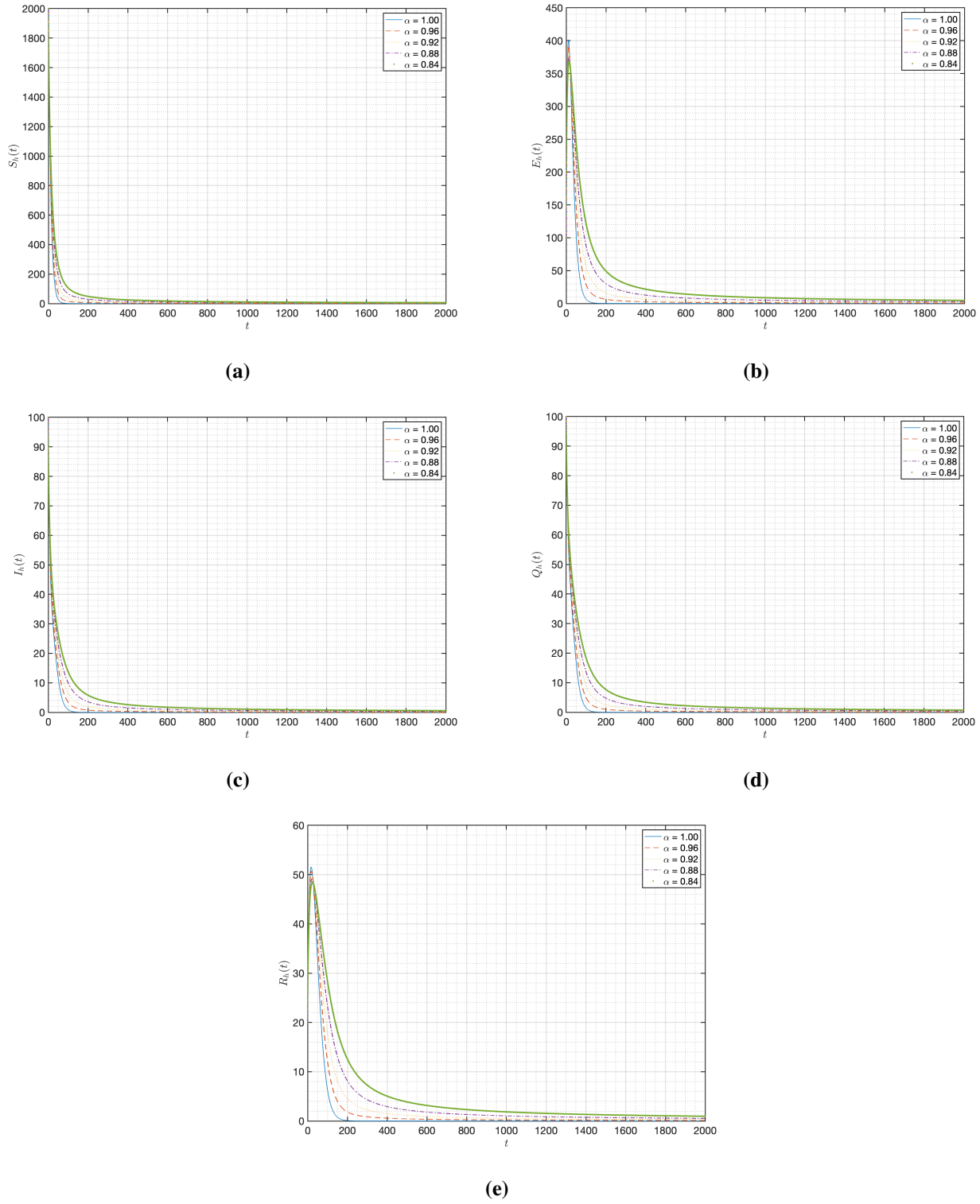

Figure 12. Numerical results of $S_h(t)$, $E_h(t)$, $I_h(t)$, $Q_h(t)$, and $R_h(t)$ of the $\mathbb{FF}$-$\mathbb{MPX}$ model (2.8) when $\alpha \in \{0.84, 0.88, 0.92, 0.96, 1.00\}$ and $\beta = 1.00$ in case of $\mathfrak{E}_1^*$.

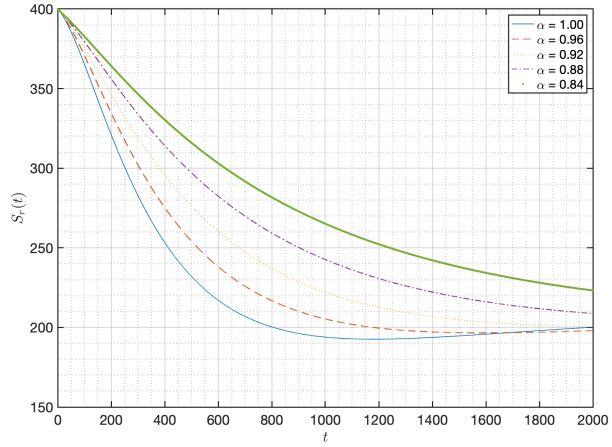

(a)

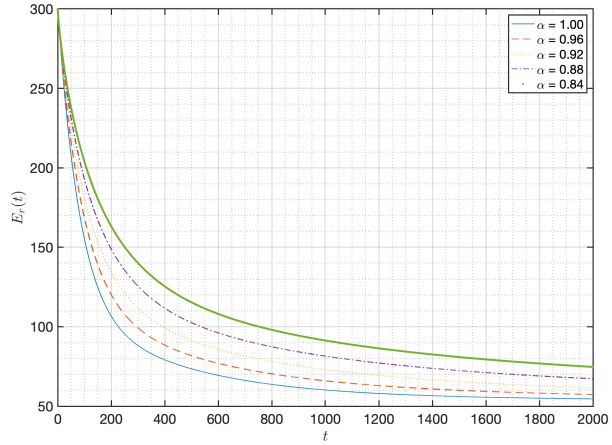

(b)

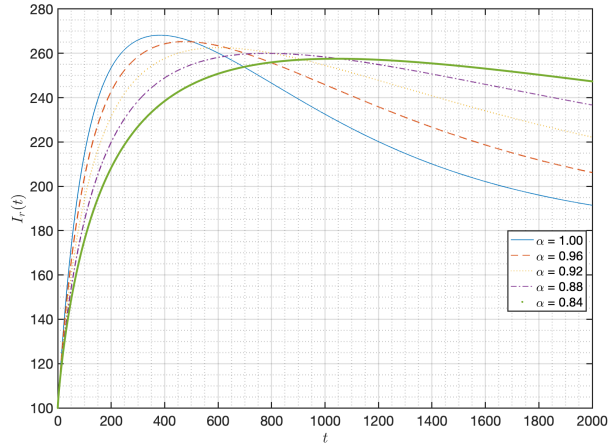

(c)

Figure 13. Numerical results of $S_r(t)$, $E_r(t)$, and $I_r(t)$ of the $\mathbb{FF}$-$\mathbb{MPX}$ model (2.8) when $\alpha \in \{0.84, 0.88, 0.92, 0.96, 1.00\}$ and $\beta = 1.00$ in case of $\mathfrak{E}_1^*$.

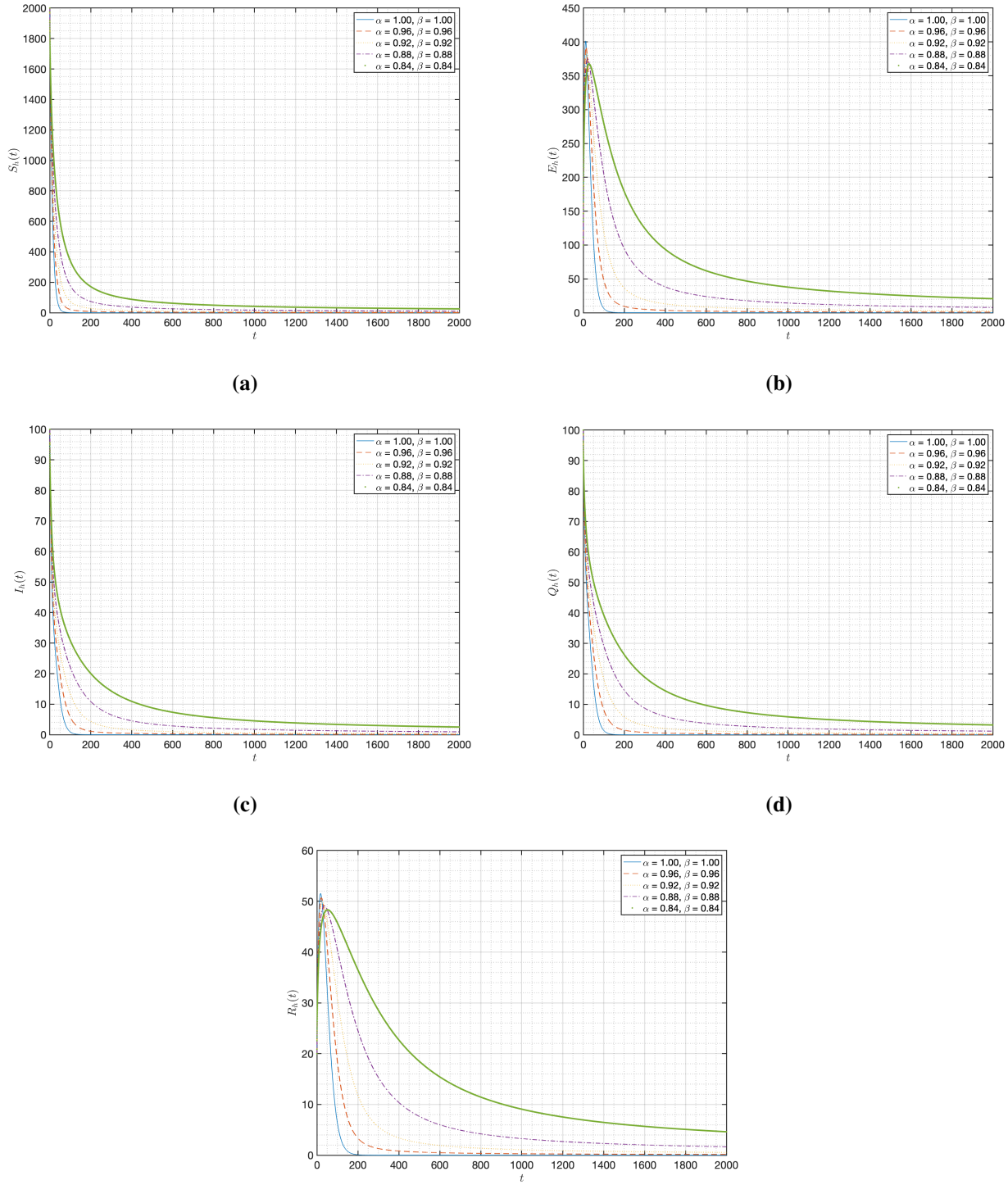

Figure 14. Numerical results of $S_h(t)$, $E_h(t)$, $I_h(t)$, $Q_h(t)$, and $R_h(t)$ of the $\mathbb{FF}$-$\mathbb{MPX}$ model (2.8) when $\alpha \in \{0.84, 0.88, 0.92, 0.96, 1.00\}$ and $\beta \in \{0.84, 0.88, 0.92, 0.96, 1.00\}$ in case of $\mathfrak{E}_1^*$.

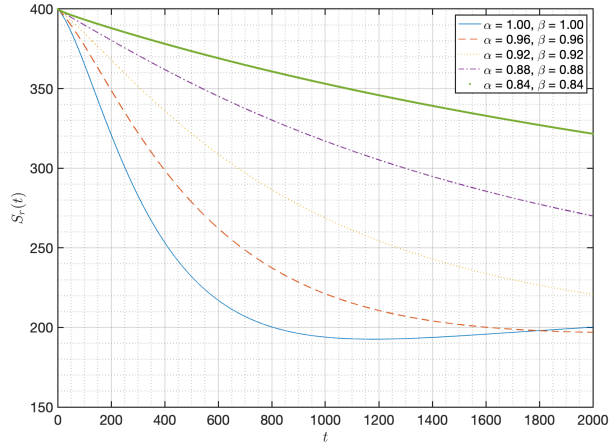

(a)

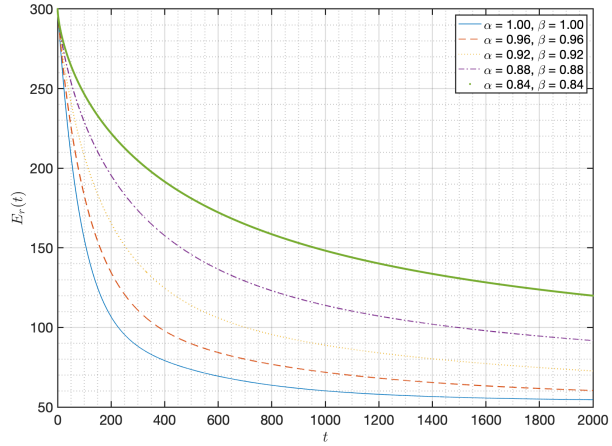

(b)

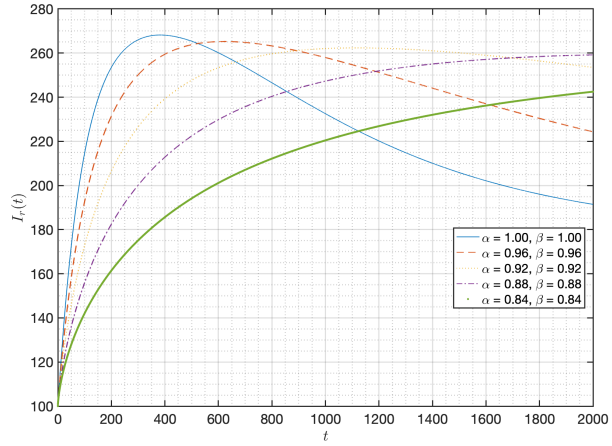

(c)

Figure 15. Numerical results of $S_r(t)$, $E_r(t)$, and $I_r(t)$ of the $\mathbb{FF}$-$\mathbb{MPX}$ model (2.8) when $\alpha \in \{0.84, 0.88, 0.92, 0.96, 1.00\}$ and $\beta \in \{0.84, 0.88, 0.92, 0.96, 1.00\}$ in case of $\mathfrak{E}_1^*$.

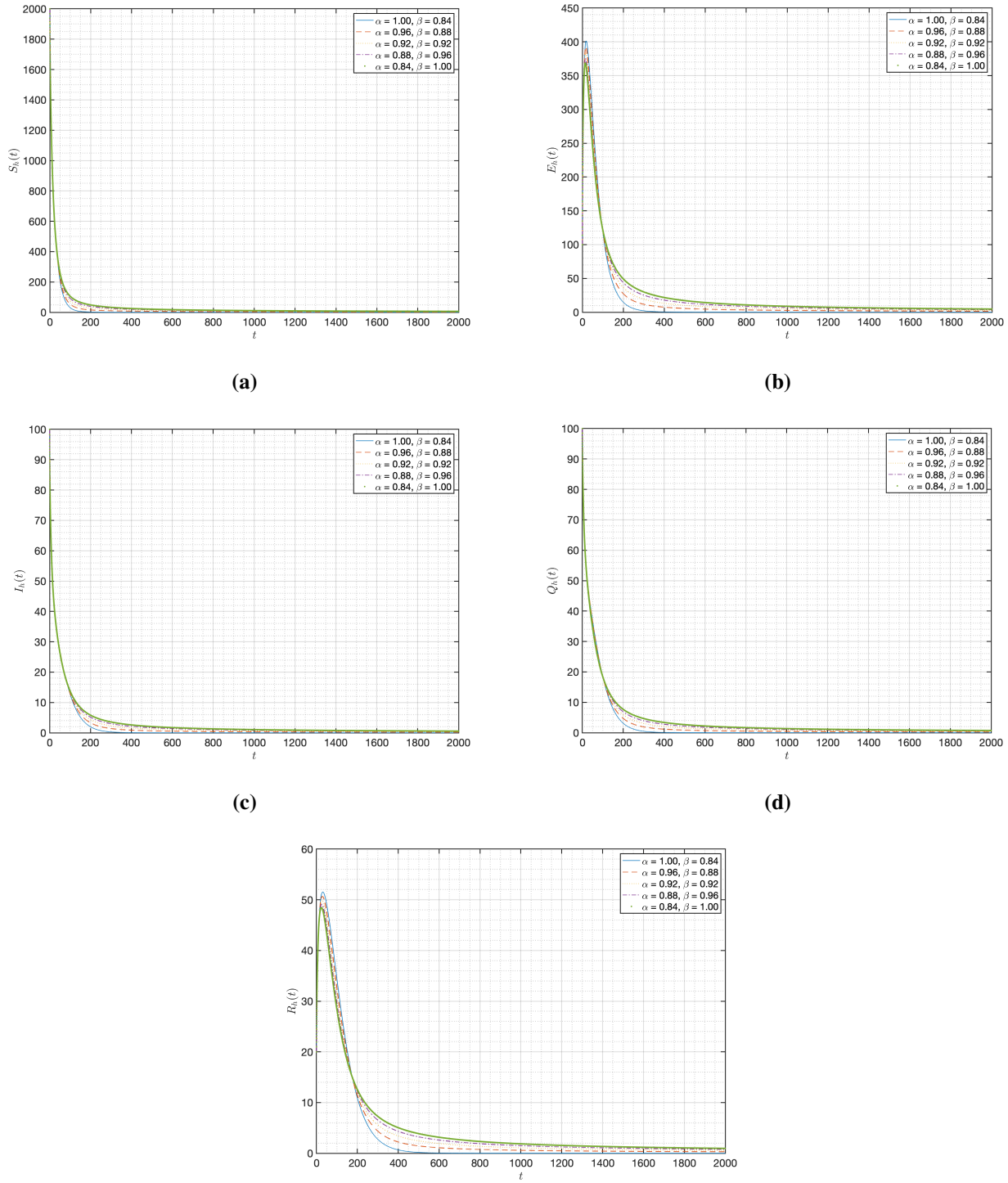

Figure 16. Numerical results of $S_h(t)$, $E_h(t)$, $I_h(t)$, $Q_h(t)$, and $R_h(t)$ of the $\mathbb{FF}$-$\mathbb{MPX}$ model (2.8) when $\alpha \in \{0.84, 0.88, 0.92, 0.96, 1.00\}$ and $\beta \in \{1.00, 0.96, 0.92, 0.88, 0.84\}$ in case of $\mathfrak{E}_1^*$.

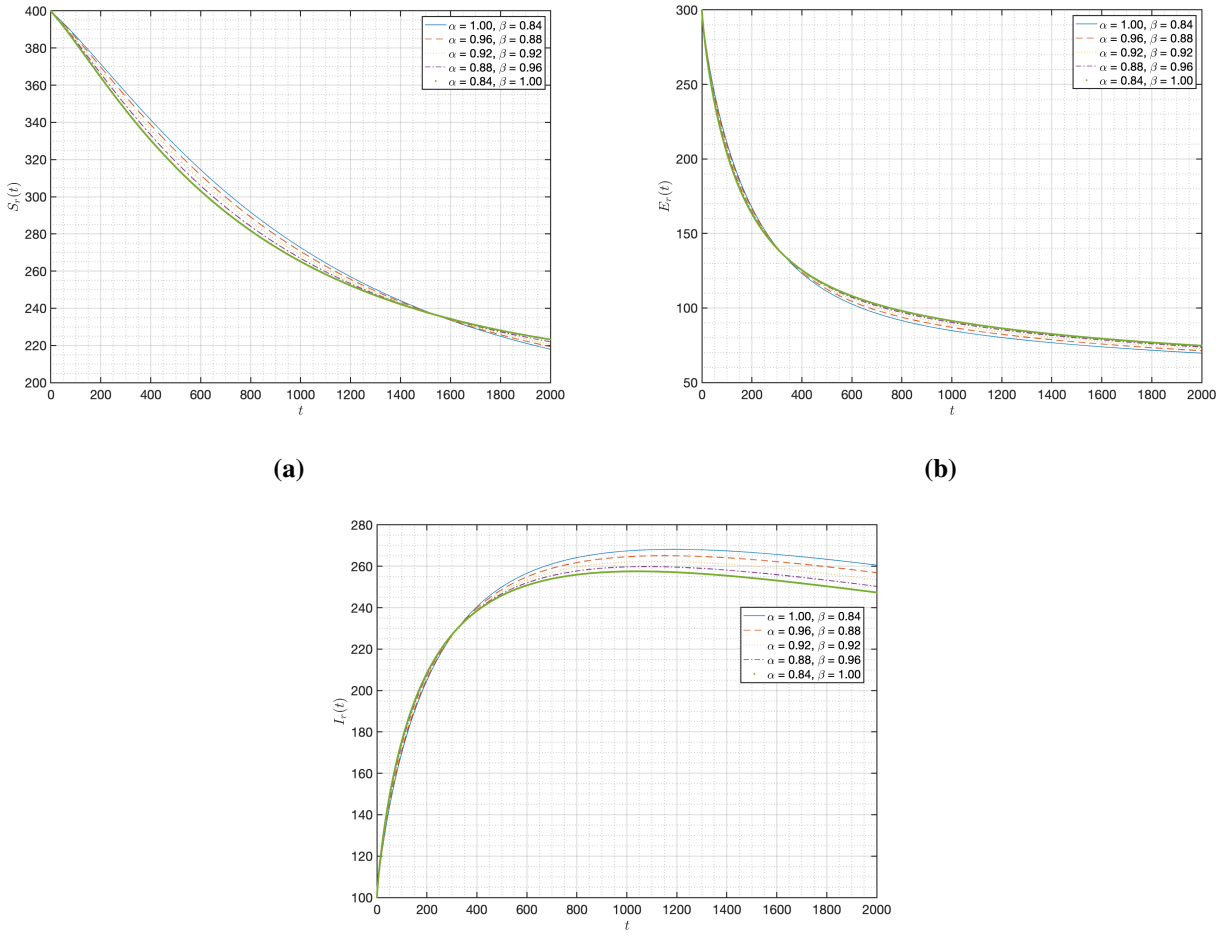

(a) **(b)**

(c)

Figure 17. Numerical results of $S_r(t)$, $E_r(t)$, and $I_r(t)$ of the $\mathbb{FF}$-$\mathbb{MPX}$ model (2.8) when $\alpha \in \{0.84, 0.88, 0.92, 0.96, 1.00\}$ and $\beta \in \{1.00, 0.96, 0.92, 0.88, 0.84\}$ in case of $\mathfrak{E}_1^*$.

7. Conclusions

In this paper, we analyzed the transmission dynamics of a deterministic mathematical model for the $\mathbb{MPX}$ virus with five human groups and three rodent groups using the $\mathbb{FF}$ operator in the context of Mittag-Leffler kernel. First, the positiveness and boundedness of the proposed model are investigated, and the equilibrium points, as well as their stability, are established. Second, the fixed point theory in the framework of Banach's and Krasnoselskii's types are used to verify the existence and uniqueness results. Third, the numerical algorithm is derived applying the Adams-Bashforth technique based on two steps of Lagrange polynomials. The numerical simulation is presented for two different cases of equilibrium points $\mathfrak{E}_0^*$ and $\mathfrak{E}_1^*$ with a variety of values α and β for some data referred to in Table 2. Finally, it can be found that the curves of the approximated solution converge to the steady state of the proposed model, which guarantees the accuracy of the results from Theorems 3.2 and 3.3. In summary, we found that the variation values of the fractal dimension and fractional order between zero and one cause a tiny effect on the dynamics of the different groups of the proposed model. The considerable

benefit of our $\mathbb{FF}$-$\mathbb{MPX}$ pandemic model is that it is more practical, efficient, and realistic than the classical model since it allows for greater flexibility, which increases precision and helps us get better results. In future research, we can consider using other fractional operators, such as piece-wise operators, stochastic operators, and so on, and apply them to the system of differential equations to analyze real-world phenomena.

Use of AI tools declaration

The authors declare they have not used Artificial Intelligence (AI) tools in the creation of this article.

Acknowledgments

This work was supported by the Faculty of Science, Burapha University, Thailand (Grant no. SC06/2565) and Ramkhamhaeng University.

Conflict of interest

The authors declare no conflicts of interest.

References

1. *Monkeypox outbreak 2022-Global,* WHO. Available from: https://www.who.int/emergencies/situations/monkeypox-oubreak-2022.
2. I. D. Ladnyj, P. Ziegler, E. Kima, A human infection caused by monkeypox virus in basankusu territory, democratic Republic of the Congo, *B. World Health Organ.*, **46** (1972), 593–597. https://www.ncbi.nlm.nih.gov/pmc/articles/PMC2480792/
3. A. Jezek, S. S. Marennikova, M. Mutumbo, J. H. Nakano, K. M. Paluku, M. Szczeniowski, Human monkeypox: A study of 2510 contacts of 214 patients, *J. Infect. Dis.*, **154** (1986), 551–555. https://doi.org/10.1093/infdis/154.4.551
4. D. A. Kulesh, B. M. Loveless, D. Norwood, J. Garrison, C. A. Whitehouse, C. Hartmann, Monkeypox virus detection in rodents using real-time 3′-minor groove binder TaqMan assays on the Roche LightCycler, *Lab Invest.*, **84** (2004), 1200–1208. https://doi.org/10.1038/labinvest.3700143
5. Y. Li, V. A. Olson, T. Laue, M. T. Laker, I. K. Damon, Detection of monkeypox virus with real-time PCR assays, *J. Clin. Virol.,* **36** (2006), 194–203. https://doi.org/10.1016/j.jcv.2006.03.012
6. V. A. Olson, T. Laue, M. T. Laker, I. V. Babkin, C. Drosten, S. N. Shchelkunov, et al., Real-time PCR system for detection of orthopoxviruses and simultaneous identification of smallpox virus, *J. Clin. Microbiol.,* **42** (2004), 1940–1946. https://doi.org/10.1128/jcm.42.5.1940-1946.2004
7. J. G. Breman, D. A. Henderson, Diagnosis and management of smallpox, *N. Engl. J. Med.,* **346** (2002), 1300–1308. https://www.nejm.org/doi/full/10.1056/NEJMra020025
8. J. G. Breman, R. Kalisa, M. V. Steniowski, E. Zanotto, A. I. Gromyko, I. Arita, Human monkeypox 1970–1979, *B. World Health Organ.,* **58** (1980), 165–182. https://www.ncbi.nlm.nih.gov/pmc/articles/PMC2395797/

9. Z. Jezek, F. Fenner, *Human monkeypox,* New York: Karger, 1988.
10. P. E. M. Fine, Z. Jezek, B. Grab, H. Dixon, The transmission potential of monkeypox virus in human populations, *Int. J. Epidemiol.,* **17** (1988), 643–650. https://doi.org/10.1093/ije/17.3.643
11. H. Meyer, R. Ehmann, G. L. Smith, Smallpox in the post-eradication era, *Viruses,* **12** (2020), 138. https://doi.org/10.3390/v12020138
12. A. W. Rimoin, P. M. Mulembakani, S. C. Johnston, J. O. L. Smith, N. K. Kisalu, T. L. Kinkela, et al., Major increase in human monkeypox incidence 30 years after smallpox vaccination campaigns cease in the Democratic Republic of Congo, *Proc. Natl. Acad. Sci.,* **107** (2010), 16262–16267. https://doi.org/10.1073/pnas.100576910
13. C. P. Bhunu, S. Mushayabasa, Modelling the transmission dynamics of pox-like infections, *IAENG Int. J. Appl. Math.,* **41** (2011), 1–9. Available from: `https://www.iaeng.org/IJAM/issues_v41/issue_2/`.
14. S. Usman, I. I. Adamu, Modeling the transmission dynamics of the monkeypox virus infection with treatment and vaccination interventions, *J. Appl. Math. Phys.,* **5** (2017), 2335–2353. https://doi.org/10.4236/jamp.2017.512191
15. S. A. Somma, N. I. Akinwande, U. D. Chado, A mathematical model of monkeypox virus transmission dynamics, *Ife J. Sci.,* **21** (2019), 195–204. https://doi.org/10.4314/ijs.v21i1.17
16. S. V. Bankuru, S. Kossol, W. Hou, P. Mahmoudi, J. Rychtár, D. Taylor, A game-theoretic model of monkeypox to assess vaccination strategies, *PeerJ,* **8** (2020), https://doi.org/10.7717/peerj.9272
17. O. J. Peter, S. Kumar, N. Kumari, F. A. Oguntolu, K. Oshinubi, R. Musa, Transmission dynamics of monkeypox virus: A mathematical modelling approach, *Model. Earth Syst. Environ.,* **8** (2022), 3423–3434. https://doi.org/10.1007/s40808-021-01313-2
18. L. E. Depero, E. Bontempi, Comparing the spreading characteristics of monkeypox (MPX) and COVID-19: Insights from a quantitative model, *Environ. Res.,* **235** (2023), 116521. https://doi.org/10.1016/j.envres.2023.116521
19. B. Liu, S. Farid, S. Ullah, M. Altanji, R. Nawaz, S. W. Teklu, Mathematical assessment of monkeypox disease with the impact of vaccination using a fractional epidemiological modeling approach, *Sci. Rep.*, **13** (2023), 13550. https://doi.org/10.1038/s41598-023-40745-x
20. A. Elsonbaty, W. Adel, A. Aldurayhim, A. El-Mesady, Mathematical modeling and analysis of a novel monkeypox virus spread integrating imperfect vaccination and nonlinear incidence rates, *Ain Shams Eng. J.*, **15** (2024). https://doi.org/10.1016/j.asej.2023.102451
21. A. A. Kilbas, H. H. Srivastava, J. J. Trujillo, *Theory and applications of fractional differential equations,* Elsevier: Amsterdam, The Netherlands, 2006.
22. M. Caputo, M. Fabrizio, A new definition of fractional derivative without singular kernel, *Prog. Fract. Differ. Appl.,* **1** (2015), 73–85.
23. A. Atangana, D. Baleanu, New fractional derivatives with non-local and non-singular kernel: Theory and application to heat transfer model, *Therm. Sci.,* **20** (2016), 763–69. https://doi.org/10.2298/TSCI160111018A
24. M. U. Rahman, Generalized fractal-fractional order problems under non-singular Mittag-Leffler kernel, *Results Phys.*, **35** (2022), https://doi.org/10.1016/j.rinp.2022.105346
25. J. Losada, J. J. Nieto, Properties of a new fractional derivative without singular kernel, *Progr. Fract. Differ. Appl.,* **1** (2015), 87-–92. https://doi.org/10.12785/pfda/010202

26. R. Kanno, Representation of random walk in fractal space-time, *Physica A,* **248** (1998), 165—175. https://doi.org/10.1016/S0378-4371(97)00422-6
27. B. Ghanbari, K. S. Nisar, Some effective numerical techniques for chaotic systems involving fractal-fractional derivatives with different laws, *Front. Phys.,* **8** (2020), 192. https://doi.org/10.3389/fphy.2020.00192
28. A. Atangana, Modelling the spread of COVID-19 with new fractal-fractional operators: Can the lockdown save mankind before vaccination? *Chaos Soliton. Fract.,* **136** (2020), 109860. https://doi.org/10.1016/j.chaos.2020.109860
29. M. Arfan, H. Alrabaiah, M. ur Rahman, Y. L. Sun, A. S. Hashim, B. A. Pansera, et al., Investigation of fractal-fractional order model of COVID-19 in Pakistan under Atangana-Baleanu Caputo (ABC) derivative, *Results Phys.,* **24** (2021), 104046. https://doi.org/10.1016/j.rinp.2021.104046
30. J. F. Gomez-Aguilar, T. Cordova-Fraga, T. Abdeljawad, A. Khan, H. Khan, Analysis of fractal-fractional malaria transmission model, *Fractals,* **28** (2020), 2040041. https://doi.org/10.1142/S0218348X20400411
31. M. Farman, A. Akgül, M. T. Tekin, M. M. Akram, A. Ahmad, E. E. Mahmoud, et al., Fractal fractional-order derivative for HIV/AIDS model with Mittag-Leffler kernel, *Alex. Eng. J.,* **61** (2022), 10965–10980. https://doi.org/10.1016/j.aej.2022.04.030
32. E. Addai, A. Adeniji, O. J. Peter, J. O. Agbaje, K. Oshinubi, Dynamics of age-structure smoking models with government intervention coverage under fractal-fractional order derivatives, *Fractal. Fract.,* **7** (2023), 370. https://doi.org/10.3390/fractalfract7050370
33. N. Zhang, E. Addai, L. Zhang, M. Ngungu, E. Marinda, J. K. K. Asamoah, Fractional modeling and numerical simulation for unfolding marburg-monkeypox virus co-infection transmission, *Fractals,* **31** (2023), 2350086. https://doi.org/10.1142/S0218348X2350086X
34. E. Addai, A. Adeniji, M. Ngungu, G. K. Tawiah, E. Marinda, J. K. K. Asamoah, et al., A nonlinear fractional epidemic model for the Marburg virus transmission with public health education, *Sci. Rep.,* **13** (2023), 19292. https://doi.org/10.1038/s41598-023-46127-7
35. H. Najafi, S. Etemad, N. Patanarapeelert, J. K. K. Asamoah, S. Rezapour, T. Sitthiwirattham, A study on dynamics of $CD4^+$ T-cells under the effect of HIV-1 infection based on a mathematical fractal-fractional model via the Adams-Bashforth scheme and Newton polynomials, *Mathematics,* **10** (2022), 1366. https://doi.org/10.3390/math10091366
36. A. Atangana, S. I. Araz, *New numerical scheme with Newton polynomial: Theory, methods, and applications*, 1 Eds, Elsevier, 2021. https://doi.org/10.1016/C2020-0-02711-8
37. V. S. Erturk, P. Kumar, Solution of a COVID-19 model via new generalized Caputo-type fractional derivatives, *Chaos Soliton. Fract.,* **139** (2020), 110280, 1–9. https://doi.org/10.1016/j.chaos.2020.110280
38. A. El. Mesady, A. Elsonbaty, W. Adel, On nonlinear dynamics of a fractional order monkeypox virus model, *Chaos Soliton. Fract.*, **164** (2022), 112716. https://doi.org/10.1016/j.chaos.2022.112716
39. M. A. Qurashi, S. Rashid, A. M. Alshehri, F. Jarad, F. Safdar, New numerical dynamics of the fractional monkeypox virus model transmission pertaining to nonsingular kernels, *Math. Biosci. Eng.*, **20** (2022), 40236. https://doi.org/10.3934/mbe.2023019

40. O. J. Peter, F. A. Oguntolu, M. M. Ojo, A. O. Oyeniyi, R. Jan, I. Khan, Fractional order mathematical model of monkeypox transmission dynamics, *Phys. Scr.*, **97** (2022), 084005. https://doi.org/10.1088/1402-4896/ac7ebc
41. A. Atangana, A. Akgu, K. M. Owolabi, Analysis of fractal fractional differential equations, *Alex. Eng. J.*, **59** (2020), 1117–1134. https://doi.org/10.1016/j.aej.2020.01.005
42. S. Qureshi, A. Atangana, A. Shaikh, Strange chaotic attractors under fractal fractional operators using newly proposed numerical methods, *Eur. Phys. J. Plus*, **134** (2019), https://doi.org/10.1140/epjp/i2019-13003-7
43. A. Granas, J. Dugundji, *Fixed point theory*, Springer: New York, 2003. https://doi.org/10.1007/978-0-387-21593-8
44. M. A. Krasnosel'skii, Two remarks on the method of successive approximations, *Usp. Mat. Nauk.*, **10** (1955), 123–127.
45. G. O. Fosu, E. Akweittey, A. S. Albert, Next-generation matrices and basic reproductive numbers for all phases of the coronavirus disease, *Open J. Math. Sci.*, **4** (2020), 261–272. https://doi.org/10.30538/oms2020.0117
46. C. P. Bhunu, W. Garira, G. Magombedze, Mathematical analysis of a two strain HIV/AIDS model with antiretroviral treatment, *Acta Biotheor.*, **57** (2009), 361–381. https://doi.org/10.1007/s10441-009-9080-2
47. M. R. Odom, R. C. Hendrickson, E. J. Lefkowitz, Poxvirus protein evolution: Family wide assessment of possible horizontal gene transfer events, *Virus Res.*, **144** (2009), 233–249. https://doi.org/10.1016/j.virusres.2009.05.006
48. M. Ngungu, E. Addai, A. Adeniji, U. M. Adam, K. Oshinubi, Mathematical epidemiological modeling and analysis of monkeypox dynamism with non-pharmaceutical intervention using real data from United Kingdom, *Front. Public Health.,* **11** (2023), 1101436. https://doi.org/10.3389/fpubh.2023.1101436
49. *Monkeypox cases confirmed in England-Latest updates*, UK Health Security Agency, 2022. Available from: `https://www.gov.uk/government/news/monkeypox-casesconfirmed-in-england-latest-updates(accessedAugust29,2022)`.